

Cleaning Verification Monitor Technique Based on Infrared Optical Methods

PP-1138

Final Report

Shane Sickafoose, David Ottesen, Douglas Scott
Sandia National Laboratories
Livermore, CA 94550

Theresa Hoffard, Daniel Polly
Naval Facilities Engineering Service Center
Port Hueneme, CA 93043

Report Documentation Page

*Form Approved
OMB No. 0704-0188*

Public reporting burden for the collection of information is estimated to average 1 hour per response, including the time for reviewing instructions, searching existing data sources, gathering and maintaining the data needed, and completing and reviewing the collection of information. Send comments regarding this burden estimate or any other aspect of this collection of information, including suggestions for reducing this burden, to Washington Headquarters Services, Directorate for Information Operations and Reports, 1215 Jefferson Davis Highway, Suite 1204, Arlington VA 22202-4302. Respondents should be aware that notwithstanding any other provision of law, no person shall be subject to a penalty for failing to comply with a collection of information if it does not display a currently valid OMB control number.

1. REPORT DATE OCT 2004	2. REPORT TYPE	3. DATES COVERED 00-00-2004 to 00-00-2004			
4. TITLE AND SUBTITLE Cleaning Verification Monitor Technique Based on Infrared Optical Methods		5a. CONTRACT NUMBER			
		5b. GRANT NUMBER			
		5c. PROGRAM ELEMENT NUMBER			
6. AUTHOR(S)		5d. PROJECT NUMBER			
		5e. TASK NUMBER			
		5f. WORK UNIT NUMBER			
7. PERFORMING ORGANIZATION NAME(S) AND ADDRESS(ES) Sandia National Laboratories, Livermore, CA, 94550		8. PERFORMING ORGANIZATION REPORT NUMBER			
9. SPONSORING/MONITORING AGENCY NAME(S) AND ADDRESS(ES)		10. SPONSOR/MONITOR'S ACRONYM(S)			
		11. SPONSOR/MONITOR'S REPORT NUMBER(S)			
12. DISTRIBUTION/AVAILABILITY STATEMENT Approved for public release; distribution unlimited					
13. SUPPLEMENTARY NOTES					
14. ABSTRACT					
15. SUBJECT TERMS					
16. SECURITY CLASSIFICATION OF:			17. LIMITATION OF ABSTRACT Same as Report (SAR)	18. NUMBER OF PAGES 47	19a. NAME OF RESPONSIBLE PERSON
a. REPORT unclassified	b. ABSTRACT unclassified	c. THIS PAGE unclassified			

TABLE OF CONTENTS

List of Figures	iii
List of Tables	v
List of Acronyms	vi
Acknowledgements	vii
Executive Summary	1
Objective	1
Project Background	2
Introduction	3
Method and Materials	4
Grazing Angle Spectroscopy	4
Tunable Infrared-Laser Imaging	7
Results and Accomplishments	11
Development of Test Coupons	11
Calibration Coupons	19
Spectral Interference	19
Non-Ideal Surfaces	23
FTIR Spectrometer Prototype Field-test Summary	26
Laser Imaging System Summary	29
Conclusions	32
Life Cycle Cost Estimate for the FTIR	35
Transition of Technology	36
References	38
Appendix	39

List of Figures

Figure 1.	Experimental arrangement and definition of important quantities in reflection-absorption spectroscopy.....	6
Figure 2.	FTIR spectrum of 0.2 μm thick film of silicone on aluminum at an angle of incidence of 30° and 75°	6
Figure 3.	Diagram of the PPLN OPO and projection optics.....	8
Figure 4.	Schematic diagram of a “fan-out” PPLN crystal, in which the period continuously varies across the crystal width. The arrows indicate the orientation of the crystallographic z-axis. In reality, the periods of inversion are much narrower than indicated (typically $\sim 29\text{-}31 \mu\text{m}$).....	9
Figure 5.	FTIR spectrum of C-H stretch absorption feature used for laser imaging. Wavelength A is used for measurement of hydrocarbon residue. Wavelength B accounts for surface reflectivity.....	10
Figure 6.	Laser image of contaminated surface at 2915 cm^{-1}	10
Figure 7.	Laser image of contaminated surface at 3000 cm^{-1}	11
Figure 8.	Laser image ratio of images in Figure 6 and 7.....	11
Figure 9.	Linear least-squares fit of experimental reflectance-absorption data for safety draw lubricant on 600 grit polished aluminum surfaces. Average film thickness: (Top) $0.9 \mu\text{m}$, (Middle) $0.4 \mu\text{m}$, (Bottom) $0.1 \mu\text{m}$	15
Figure 10.	Integrated reflection-absorption intensity at 60° angle of incidence for C-H stretching bands of Safety Draw films deposited on aluminum test coupons with varying degrees of surface roughness (longitudinal, top; transverse, bottom).....	16
Figure 11.	Integrated reflection-absorption intensity at 75° angle of incidence for C-H stretching bands of Safety Draw films deposited on aluminum test coupons with varying degrees of surface roughness (longitudinal, top; transverse, bottom).....	17
Figure 12.	Initial reflection-absorption intensities of C-H stretching bands for Cosmoline films deposited on aluminum test coupons with varying degrees of surface roughness.....	18

Figure 13.	Potential interference effects of water on C-H stretching bands due to hydrocarbon contaminants. Three thicknesses of water film are examined (1 μm , top; 3 μm , middle; and 7 μm , bottom).....	20
Figure 14.	Comparison of infrared reflection spectra for hydrocarbon-contaminated aluminum surfaces from NAVDEP North Island (etched and deoxidized – top; chromate-conversion coated – middle; sulfuric acid anodized – bottom).....	21
Figure 15.	False-color reflectance-ratio images of NAVDEP chromate conversion aluminum surfaces contaminated with a hydrocarbon soil mixture: 40.5 $\mu\text{g}/\text{cm}^2$ (top), 28.1 $\mu\text{g}/\text{cm}^2$ (middle), and 14.3 $\mu\text{g}/\text{cm}^2$ (bottom) average surface deposit.....	22
Figure 16.	FTIR reflectance spectra for Cosmoline on aluminum cylinders (1-cm radius) at 75° angle of incidence and longitudinal orientation.....	24
Figure 17.	FTIR spectra of a 0.2 μm Cosmoline film on aluminum cylinder at 75° and 60° angle-of-incidence for transverse and longitudinal beam orientations.....	24
Figure 18.	Integrated peak area for Cosmoline on aluminum cylinder at a 75° angle of incidence as a function of film thickness.....	25
Figure 19.	Integrated peak areas of the 1735 cm^{-1} band in the FTIR reflectance spectra of aluminum panels contaminated with Partall Film #10 as a function of angle-of-incidence.....	25
Figure 20.	False-color laser-image ratios for Cosmoline contaminated cylindrical surfaces: 89.3 $\mu\text{g} / \text{cm}^2$ (top) and 20.4 $\mu\text{g} / \text{cm}^2$ (bottom) average surface deposit.....	27
Figure 21.	Portable FTIR analyzing (A) C130 bare aluminum belly and (B) an area containing yellow epoxy primer on an F-16.....	28
Figure 22.	FTIR operator at the C130 demonstrating handheld FTIR operation.....	29
Figure 23.	FTIR operating on a camera tripod to analyze the F-16.....	29
Figure 24.	The new thermoelectrically-cooled silicon microbolometer array with attendant electronics.....	31
Figure 25.	A screen capture of the control and data analysis software developed in conjunction with the microbolometer array.....	31

Figure 26. Economic Analysis of the FTIR spectrometer for a specific
DOD cleaning application..... 36

List of Tables

Table 1. Test materials chosen for evaluation of technique..... 12

List of Acronyms

AFB = Air Force Base

cw = continuous wave

DAC = Defense Ammunition Center

DOD = Department of Defense

DOE = Department of Energy

EM = Energetic Material

FTIR = Fourier Transform Infrared Spectroscopy

HMX = 1, 3, 5, 7-tetranitro-1, 3, 5, 7-tetrazacyclooctane

IR = Infrared

IRRAS = Infrared Reflection-Absorption Spectroscopy

MOU = Memorandum of Understanding

NASA = National Air and Space Administration

NAVDEP = Naval Depot

Nd:YAG = Neodymium doped, Yttrium-Aluminum-Garnet

NFESC = Naval Facilities Engineering Services Center

N.I. = North Island, Naval Depot

NPV = Net Present Value

OPO = Optical Parametric Oscillator

PP = Pollution Prevention

PPLN = Periodically-Poled Lithium Niobate

PPSON = Pollution Prevention Statement of Need

QPM = Quasi-Phasematching

RDX = hexahydro-1, 3, 5-trinitro-s-triazine

RSG = Sandia National Laboratories' Remote Sensing Group

SERDP = Strategic Environmental Research and Development Program

SOC = Surface Optics Corporation, Inc.

SON = Statement of Need

TAC = Technical Advisory Committee

TNT = 2, 4, 6-trinitrotoluene

TTAWG = Technical Thrust Area Working Group

VOC = Volatile Organic Compound

ACKNOWLEDGMENTS

The results of this project represent the efforts of many people, not just the list of authors. The project was the brainchild of David Ottesen, who retired partway through the project. He provided leadership and technical knowledge to all aspects of the project. Other people performed a great deal of the laboratory and engineering work and spent hours tweaking lasers and optics, generating samples, and, most importantly, providing advice.

Several Post-Doctoral Appointees at Sandia National Laboratories/Livermore aided in the initial experiments for proof of concept and the transition of the laser technology from the gas-phase imaging system to this condensed phase system; these include Scott Robinson, Pete Ludowise, and Uta Goehrs. Two technologists at Sandia proved invaluable in keeping the project on track and for providing continuity, Howard Johnsen and Joseph Loomis. The laser source, which forms the basis of the laser imager, would not exist without earlier work by Scott Bisson and Thomas Kulp. Richard Shagam's insights on arrangement of the camera lens and detector for the grazing angle setup were crucial in getting the laser prototype to the stage that it currently is. Sarah Allendorf provided helpful discussion during the early stages of the project.

The excellent scientists and engineers at Surface Optics Corporation facilitated development of both IR instruments. Martin Szczesniak headed the project for construction and commercialization of the portable FTIR instrument. Mark Dombrowski, Phillip Mattison, and Kevin Dumber provided the thermoelectrically-cooled silicon microbolometer and the integrated control software for the laser imager.

All of the field tests ran smoothly because of the friendly, helpful, and efficient personnel at North Island Naval Depot and Hill Air Force Base.

Finally, we gratefully acknowledge the financial support for these investigations by the Department of Defense through the Strategic Environmental Research and Development Program (SERDP).

Executive Summary

This is the final report in the development of two real-time non-contacting monitors for cleaning verification based on infrared optical methods. New analytical capabilities are required to maximize the efficiency of cleaning operations at DOD facilities, thus reducing waste streams generated while improving the quality of subsequent processes and the long-term reliability of repaired or refurbished parts. These methods will also be of great use for similar activities in DOE and commercial sector applications.

During the course of the project we developed, built, and transitioned into the commercial sector a portable grazing-angle reflectance Fourier transform infrared (FTIR) spectrometer. We also developed a prototype for a tunable infrared-laser imaging instrument. Both can be applied on-line as real-time methods for the detection of contaminant residues common to DOD components. While both methods rely on the technique of infrared reflection spectroscopy for the detection of residues, each offers unique capabilities that can be used in either independent or complementary modes of operation.

Three field tests of the prototype FTIR instrument were performed, two at Hill Air Force Base, Ogden, Utah and one at North Island. Following completion of the modifications suggested during the first and second field tests, a final field test was conducted at Hill AFB in March 2002. The current version of the prototype is commercially available and at least three units sold to Boeing Corporation, NASA, and Oak Ridge National Laboratory.

Construction of the laser prototype continued to an intermediate point. A portable version of the spectrometer was constructed, but personnel, equipment, and funding limitations prevented development of a truly man portable version of the spectrometer and a transition of the prototype to commercialization.

Objective

Sandia National Laboratories, Livermore, CA, partnered with the Naval Facilities Engineering Service Center (NFESC), Port Hueneme, CA, and Surface Optics Corporation, San Diego, CA, in the development of two prototype instruments with complementary capabilities for cleaning verifications. In each case, surface contamination is detected by its absorption of a grazing-incidence infrared beam reflected from the surface. The instruments differ in the nature of the information they provide. The laser-based instrument produces images that directly indicate the spatial extent and location of hydrocarbon contamination. The FTIR instrument provides a wide-band spectral measurement of the surface reflectance at a single point for nearly all organic materials, and many inorganic components. Thus, the imaging system will allow rapid determination of the cleanliness of an entire surface for organic residues, while the spectrally-resolved method will be useful in identifying the specific molecular composition of a contaminant at the expense of spatial information and speed.

Sandia led the development of an imaging system that employs a widely tunable infrared laser in conjunction with an infrared camera. This approach provides an on-line technique for surveying contamination levels over large surface areas in a real-time imaging mode. The laser is broadly-tunable over the 1.3-4.5 μm wavelength range, thus allowing the detection of many hydrocarbon contaminants via their CH-, OH-, and NH-stretch absorptions. NFESC prepared characterized samples for analysis.

NFESC led the concurrent development of the wide-band spectral instrument using FTIR reflectance spectroscopy. While FTIR is a mature analytical technique, previously available commercial instrument configurations were not well suited for real-time analysis of surface contaminants at very low levels of concentration. A modified prototype instrument was developed and field-tested during the third year of this project that was optimized for the identification of a broad-range of organic and inorganic contaminants on component surfaces under field operational conditions. Sandia participated in the development of the design of the grazing-angle reflectance instrument, while Sandia and NFESC jointly identified DOD applications, customers and sites for field evaluation.

Background

In this project we addressed SERDP Pollution Prevention Statement of Need PPSON-99-03, "Cleaning Verification Techniques." Real-time methods to provide both qualitative and quantitative assessments of surface cleanliness are needed for a wide variety of military applications. The availability of a convenient analysis technology for on-site, post-cleaning determination of surface contamination will allow more rapid and accurate assessments of the efficiency of chosen cleaning techniques. Overall, this capability will lead to the reduction of hazardous materials usage, handling and disposal, and to improved alternative cleaning products and processes.

The range of DOD sites needing such a technology is large with primary applications focusing on aircraft component surfaces to be coated, plated or bonded. Additional miscellaneous applications include the examination of shipboard surfaces for mounting of absorbing tiles, bearing refurbishment; and cleaning of valve seals, gyroscope housings, and various electronic components. By developing an on-line technique, the analysis will not need to be done remotely, and processed parts will not have to be sent to a separate laboratory for analysis, thereby eliminating processing delays. The information provided by the developed optical methods can assist process operators in determining subsequent actions to be taken, as well as aid in distinguishing between specific contaminants.

During the course of the project, two prototype infrared-optical instruments were developed for use at DOD sites to reduce the use, emission and handling of hazardous materials in cleaning operations, and are applicable to DOE and commercial sector needs. The instruments are complementary in nature, and primarily used for the real-time on-line detection of contaminant residues on reflective surfaces.

One prototype infrared-optical instrument has been developed, field-tested, and is commercially available, the grazing-angle reflectance FTIR instrument. The second instrument, the laser-based prototype, underwent preliminary prototype construction and laboratory testing.

Other methods, such as the “Visual Cleaning Performance Indicator” (VCPI) approach being led by Battelle (SERDP PP-1117), utilize visible dyes and chemical coupling agents to form an adherent complex that reveals the presence of many surface contaminants. This approach has the advantages of simplicity and low cost, but is not capable of identifying molecular species and may be severely limited in yielding quantitative measurements. The effect of the dye and coupling agents on subsequent surface characteristics has not been evaluated. The combination of our non-contact optical measurements and the chemical detection VCPI method offer a wide range of complementary capabilities in real-time surface cleanliness verification.

Introduction

Currently, the detection and identification of surface contaminants on reflective surfaces is accomplished most conveniently and rapidly by Fourier transform infrared (FTIR) reflectance methods. These non-destructive, non-contact optical techniques identify the chemical constituents of the contaminants, and can yield quantitative measurements with appropriate calibration. Infrared optical methods are particularly useful for cleanliness analysis since the surface is probed under ambient conditions. As a result, the method is amenable to on-line usage, although it has insufficient sensitivity to detect the sub-monolayer quantities detectable by various high-vacuum electron and ion spectroscopic techniques (X-ray photoelectron spectroscopy, Auger electron spectroscopy, and secondary-ion mass spectrometry).

A highly desirable characteristic of a cleaning verification instrument is the ability to rapidly survey large surface areas and to determine the location and extent of any remaining contaminant following cleaning operations. Our laser-based instrument offers this capability for hydrocarbon species due to characteristic C-H stretching absorption bands in the 3- μm wavelength region. In contrast, an FTIR-based infrared reflectance analysis is able to characterize a very broad range of organic constituents and many inorganic species. However, a surface-probing FTIR instrument measures a spectrum at only a single small area on a sample, thus requiring broad area surveys to be done by sequentially probing many points. Even at a characteristic data rate of ~ 1 measurement point per second, this can be a time-consuming process. The rate of measurement by an FTIR is constrained by the relatively low spectral brightness (compared to a laser) of the incandescent illumination sources used in an FTIR instrument. This makes it necessary to use relatively long integration times to achieve an acceptable signal-to-noise ratio.

The tunable-laser-based instrument overcomes these limitations by instantaneously imaging a broad surface area during illumination by a high-brightness infrared laser. These single-

wavelength reflectance measurements are made on a timescale of 1/30th of a second. Multiple wavelength measurements are acquired by tuning the laser and repeating the image acquisition at each desired wavelength. While a detailed spectral map of a surface can be generated over the laser tuning range, the primary use of the system is to provide rapid area surveys at a few key wavelengths that are indicative of hydrocarbon contaminants.

We used a broadly-tunable infrared laser illuminator in conjunction with an infrared imaging camera. This work benefited from technology developed for other applications in Sandia's Remote Sensing Group (RSG). The RSG exploited a new breakthrough in infrared laser technology, called quasi-phases matching (QPM), to increase the tuning range and power of the infrared light source while reducing its size. The quasi-phases matching technique has been successfully used in the RSG to generate tunable infrared laser light for natural gas emission imaging and for developing laser-based spectroscopic gas sensors. We leveraged this expertise to extend the technique to detection of hydrocarbon residues on material surfaces. The approach developed can evaluate component cleanliness, as well as reveal the location of high contaminant concentrations, thus permitting localized cleaning on-line with further reduction in solvent usage.

The prototype IR-laser imaging instrument developed in this project is limited in the identification of specific organic surface contaminants due to the tuning range of the laser source. The current tuning range of the laser-based system is limited at long wavelengths to about 4.5 μm . This limits the sensitivity of the chemical imaging system primarily to functional groups containing hydrogen atoms (C-H, N-H, O-H). For this reason, we have developed a prototype instrument based on FTIR reflectance spectroscopy despite its limitations in rapidly characterizing large surface areas (discussed above).

Throughout the project, samples were prepared at NFESC for analysis with grazing-angle reflectance by both FTIR and tunable-infrared-laser methods. The much larger bandwidth of the FTIR instrumentation provides a measure of achievable sensitivity for a variety of organic contaminants. FTIR was used to validate measurements by the laser-based instrument. In turn, the spatial resolution capabilities of the PPLN-laser imaging system can visualize the uniformity of contaminants on prepared samples, and aided the quantitative understanding of spatially integrated FTIR measurements.

Several key points had to be evaluated to gauge the potential success of the two prototypes, they are: fundamental spectroscopic detection limit, spectral interference, ability to handle non-ideal surfaces, and portability.

Methods and Materials

Grazing Angle Spectroscopy

FTIR reflectance spectroscopy permits the detection of the full range of organic, and some inorganic, contaminants on a variety of reflective surfaces, and is one of the simpler methods for cleaning verification. Previously, available commercial instruments based on the infrared

reflectance method by Foster-Wheeler / Sensiv and Surface Optics Corporation for surface analysis of coatings and cleanliness conveniently provided both quantitative and qualitative information on surface coatings. They were, however, greatly limited in ultimate sensitivity to surface contaminants by the nature of their optical design. Infrared radiation was focused onto the surface to be analyzed at a near-normal angle of incidence, resulting in a compact hand-held design. The sensitivity of the instrument to very thin layers of surface species was severely limited, however, due to poor coupling of the incident electromagnetic field with the vibrating dipoles of the surface molecular species [1-3] in layers less than 0.1 μm thick.

In order to maximize the sensitivity of infrared reflectance measurements for absorption bands in thin layers on metallic surfaces, theoretical and experimental studies [4, 5] have shown that the angle of incidence of infrared radiation on the surface should be increased to at least 60°. This is also true for many impurities on the surface of non-metals, such as dielectrics and semiconductors (although the detectability of contaminant absorption bands under these circumstances depends strongly on the optical constants of both surface and substrate, and any absorption features intrinsic to the non-metallic substrate). Additional sensitivity in the reflection measurement is obtained by measuring only the reflected component of the infrared radiation polarized parallel to the plane of incidence. This collective approach is variously referred to as, “grazing-angle” spectroscopy or infrared reflection-absorption spectroscopy (IRRAS).

Grazing-angle reflectance spectroscopy underlies both the FTIR and tunable laser-imaging methods being developed in this project. The general approach has been discussed in the literature [1, 2] and is outlined in Figure 1 for an infrared beam incident on a contaminant-laden surface. In this diagram, polarization components (s, p) are shown along with film thickness (d) and angle of incidence (Θ).

As discussed above, grazing-angle incidence reflectance spectroscopy acts to enhance detection sensitivity for thin layers of residue predominantly through improved coupling of the electric field intensity of the incident beam with the vibrating dipoles of the surface layer (contaminant). Some additional enhancement of the infrared absorption spectrum will also occur due to a lengthening of the effective path length through the absorbing thin film layer.

Displayed in Figure 2 is the FTIR spectrum of a sample of a 0.2 μm silicone film with the incident beam at 30° and 70° from normal. The signal enhancement is dramatic.

Such a method also allows for the analysis of significantly larger and irregularly shaped samples, such as are commonly encountered in DOD applications. Sampling accessories for grazing-angle reflectance analysis within FTIR sample compartments are commercially available and the intrinsic methodology is established.

Joint NFESC / EPA investigations successfully used FTIR diffuse reflectance measurements to demonstrate the superiority of new aqueous solvents over trichloroethylene degreasing for the removal of hydrocarbon lubricants from aluminum substrates [6, 7]. However, the sensitivity of these measurements to the presence of very thin lubricant residues was limited

by the diffuse reflectance technique. Previous studies at Sandia [8] have shown that very thin layers of surface contaminants are

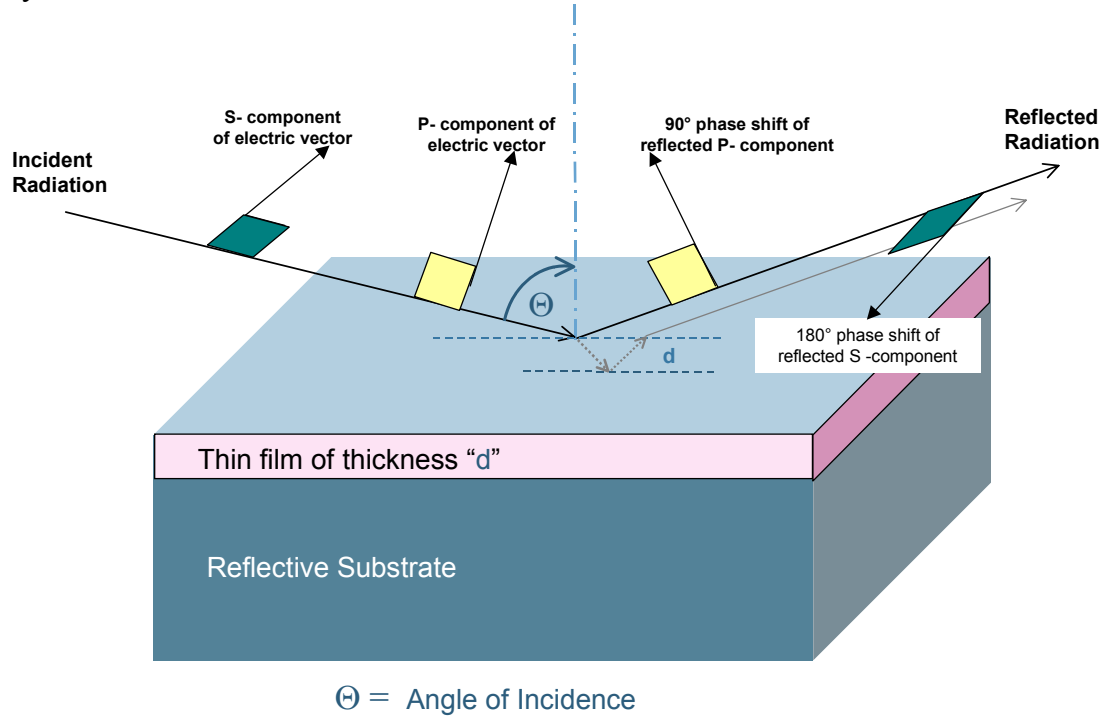


Figure 1. Experimental arrangement and definition of important quantities in reflection-absorption spectroscopy.

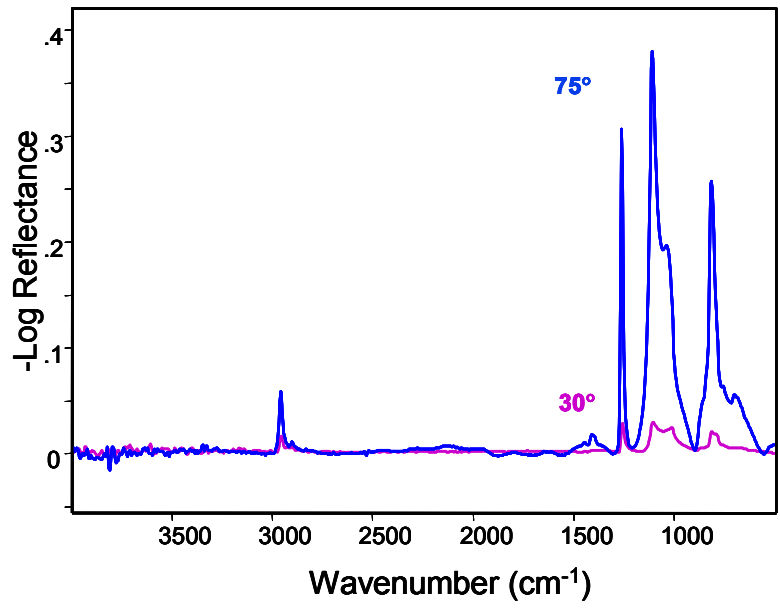


Figure 2. FTIR spectrum of $0.2 \mu\text{m}$ thick film of silicone on aluminum at 30° and 75° angle of incidence.

detectable by the grazing-angle infrared reflectance method, and that this approach is useful in alleviating problems encountered in adhesive bonding or welding operations, chemical passivation of surfaces, and the functioning of valve components.

Tunable Infrared-Laser Imaging

While the FTIR system makes use of a traditional IR source and detector, the laser imaging system makes use of a novel development in tunable IR laser sources. We use an optical parametric oscillator (OPO) that is pumped by a continuous-wave (cw) Nd:YAG laser. An OPO is a laser-like device that consists of a nonlinear crystal contained within an optical cavity (see Figure 3). In the present system, the OPO crystal is periodically-poled lithium niobate (PPLN) [9]. During operation, it is driven by the electric field of the pump laser, causing the formation of two new laser beams whose frequencies add to that of the pump laser. The reflectivities of the mirrors in the optical cavity are selected to resonate one of the generated waves, while the other wave is simply generated and released from the cavity. The resonated wave is called the signal; the non-resonated wave is called the idler. The exact frequencies of the signal and the idler are determined by the phasematching properties of the crystal, the reflectivity of the cavity, and by any spectrally-selective optics that may be placed in the cavity. While either the signal or the idler beams can be used for measurements, only the idler is used in the experiments to date.

The use of the quasi-phasematched (QPM) material PPLN makes cw OPO operation more tunable and efficient than it would be for a conventional birefringently phasematched crystal. Simply stated, phasematching is a condition in which all of the interacting waves (i.e., signal, pump, and idler) maintain a specified relative phase relationship as they propagate through a nonlinear medium, and is a necessary condition for efficient nonlinear generation. In birefringent materials, phasematching is achieved by careful selection and/or control of the crystal birefringence, temperature, and beam propagation angles.

In a QPM medium, phasematching is engineered into the medium by causing the crystal to have a periodically inverting optical axis (see Figure 4). The engineering process increases conversion efficiency by allowing the use of much stronger nonlinear coefficients of the crystal, and frees the system from reliance on birefringence, thereby increasing tunability. As the light beams cross the crystal-axis-inverting boundaries, any relative dephasing of the waves is corrected. For a crystal of a given periodicity, the rephasing is effective for a particular set of pump, signal, and idler frequencies. Some degree of tuning of these waves can be achieved within the crystal phasematching bandwidth (typically 10-20 cm^{-1}). Broader tuning is achieved by accessing a portion of the same crystal having a different periodicity, or by changing the temperature of the crystal. The “fanout” grating in Figure 4, for example, allows the periodicity to be continuously changed by translating the crystal through the pump laser beam.

In the present laboratory system, two 50-mm-long PPLN crystals (Crystal Technology) with an aperture of 11.5mm×0.5mm are used as the active medium. Each contains eight poled regions having different periodicities. When operating at a crystal temperature of 148° C,

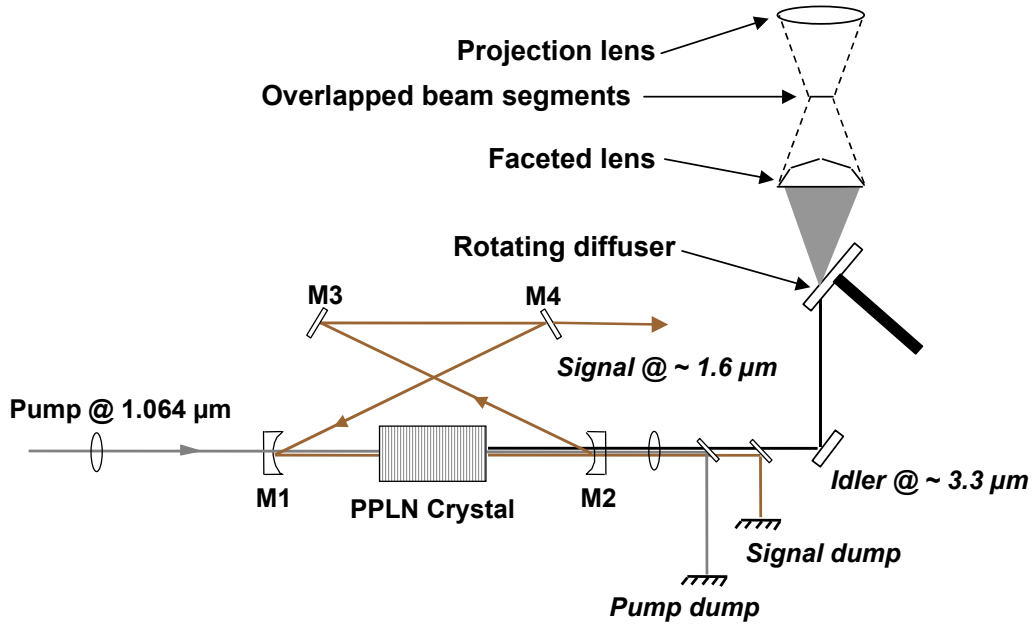


Figure 3. Diagram of the PPLN OPO and projection optics.

these periods collectively allow tuning of the idler from 2720 to 3702 cm^{-1} . The crystals are mounted in a stacked fashion within a temperature-stabilized copper oven that is attached to a vertical translation stage. Each crystal is tuned by selecting a period using the vertical motion of the stage; horizontal motion of the oven is used to select one crystal or the other.

As shown in Figure 3, the OPO used in the imaging sensor is of the “bowtie-ring” design. A diode-pumped, cw, multimode Nd:YAG laser (Lightwave Electronics) that is capable of generating at least 11 W of output power at 1064 nm is used as the OPO pump source. Two flat mirrors (M3 and M4) and two curved mirrors (M1 and M2, 50-mm radius of curvature), all coated to be highly reflective at the signal and highly transmissive at the pump and idler wavelengths, form the bow-tie-shaped singly resonant ring oscillator designed to resonate the signal wave. An anti-reflection-coated lens, positioned between the pump laser and the OPO cavity, serves to image the gaussian pump beam into the PPLN crystal. In this way, a beam waist (E-field radius) of $70 \mu\text{m}$ is created in the center of the crystal, which itself is centered between the two curved cavity mirrors. During normal operation, the OPO resonates on a single signal mode for minutes at a time, whereupon it hops to another cavity mode. The idler bandwidth is, however, determined by that of the pump beam, which is $10\text{--}15 \text{ GHz}$.

The raw output of the OPO contains the idler beam as well as portions of the signal and pump beams and some higher-order (red, green) beams created spuriously in the PPLN crystal. Spectral filtering is used to dump all but the idler beam. Prior to illumination of the sample, the idler is passed through a set of projection optics. The first of these is a ZnSe diffuser (mean roughness of $\sim 3\text{-}4\ \mu\text{m}$) that is mounted on a motor-driven spindle. The diffuser serves to destroy the phase coherence of the idler to minimize laser speckle noise in the transmitted beam and in the reflected light viewed by the IR camera. The cone of radiation leaving the diffuser is collected by a ZnSe faceted lens (Laser Power Optics). The faceted lens forms an expanded beam that is segmented into 32 different square beamlets that are subsequently overlapped at a distance of 2" from the surface of the lens. The square-shaped overlap region is then imaged onto the target converting the Gaussian profile of the idler beam into a uniform square illumination on the sample surface.

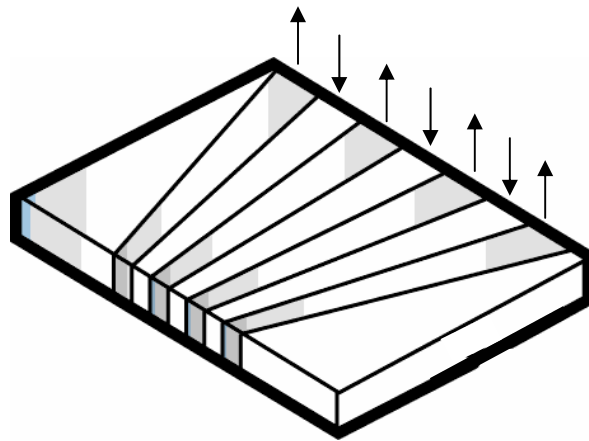


Figure 4. Schematic diagram of a “fan-out” PPLN crystal, in which the period continuously varies across the crystal width. The arrows indicate the orientation of the crystallographic z-axis. In reality, the periods of inversion are much narrower than indicated (typically $\sim 29\text{-}31\ \mu\text{m}$).

The infrared laser light is incident on the sample surface at an angle of 60° from the surface normal, and the reflected component is detected by a Silicon microbolometer array with an infrared macro-lens assembly and an array size of 320×240 pixels. The microbolometer is located approximately 0.1 m from the sample surface, and the resulting field of view is 20×35 mm. A balance between imager’s field-of-view and compactness of the detector system is required in order to ensure that the prototype is easily manageable by workers in the field.

The typical laser image is collected by tuning the wavelength of the laser to the maximum absorption of the hydrocarbon, for the suite of materials examined this maximum was near $2915\ \text{cm}^{-1}$. An image is collected at this wavelength, typically by averaging 20 different 60 microsecond exposures. Then the laser was tuned off of the absorption feature, near $3000\ \text{cm}^{-1}$ and a second image was collected. The ratio of these two images is created and

normalized by the average image ratio of a clean surface taken at the same wavelengths. The relative positions of these wavelengths can be seen in Figure 5.

Figure 6 is the image collected of a contaminated surface with the laser tuned to wavelength A in Figure 5. Figure 7 is an image of the same contaminated surface with the laser tuned to the wavelength denoted by B in Figure 5. Figure 8 is the false-colored image created by the ratio of Figure 5 versus Figure 6. The false color aids interpretation. Through the use of calibration coupons, the false color scale or the gray scale images can represent quantitative levels.

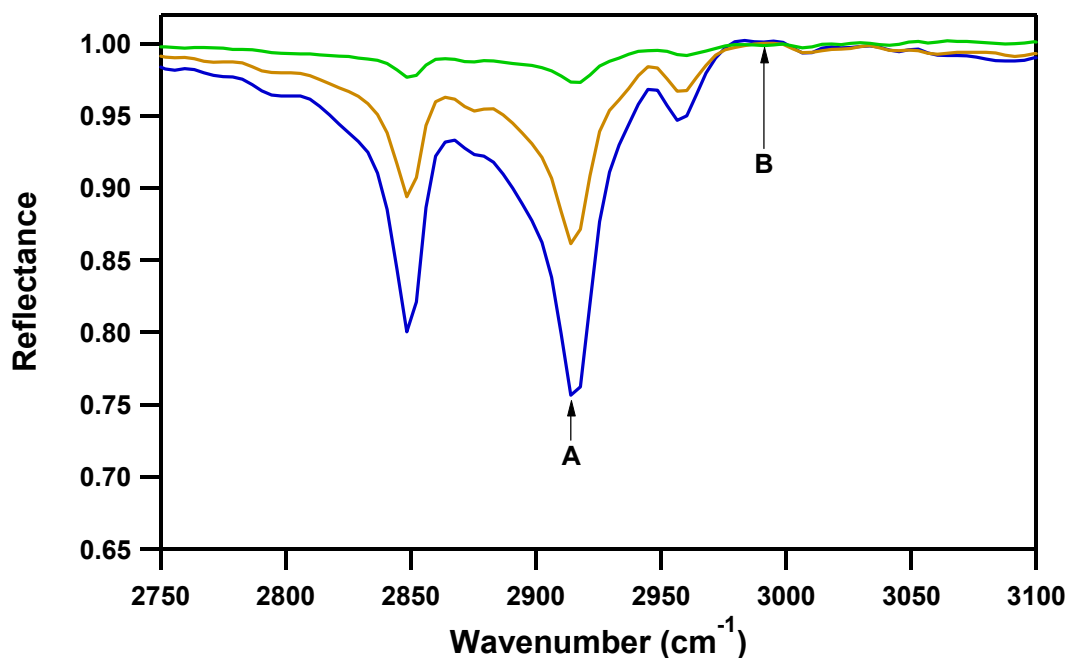


Figure 5. FTIR spectrum of C-H stretch absorption feature used for laser imaging. Wavelength A is used for measurement of hydrocarbon residue. Wavelength B accounts for surface reflectivity.

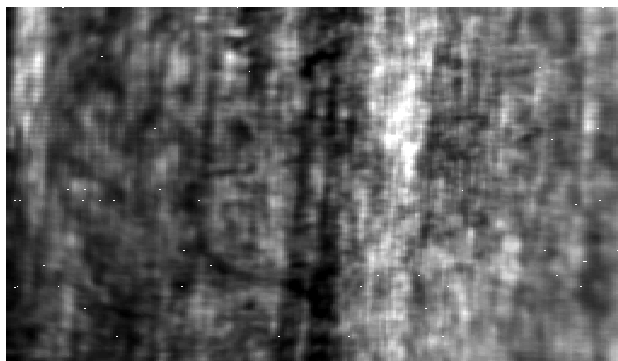


Figure 6. Laser image of surface contaminated with Safety Draw with laser tuned to 2915 cm⁻¹.

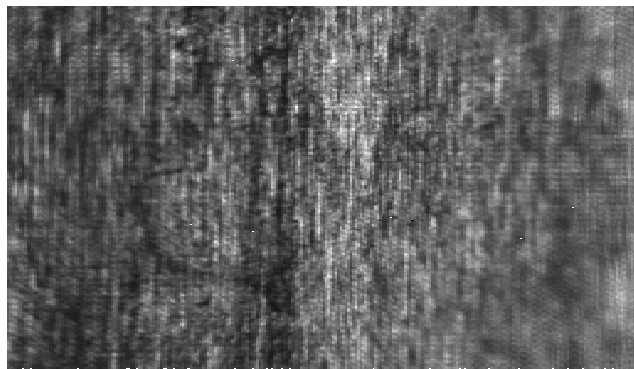


Figure 7. Laser image of surface contaminated with Safety Draw with laser tuned to 3000 cm^{-1} .

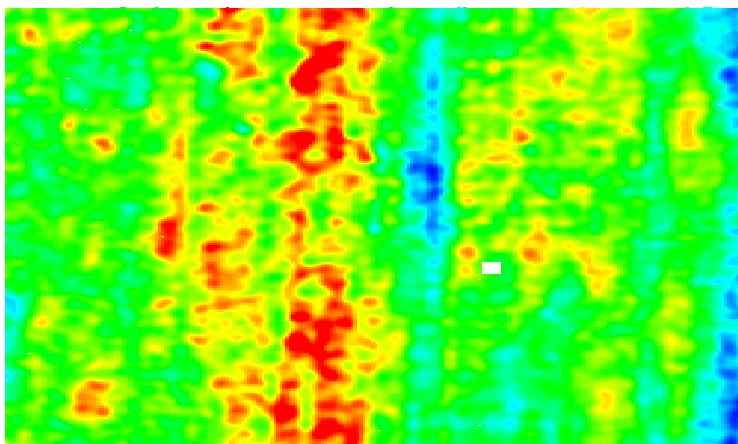


Figure 8. Ratio of laser images seen in Figures 6 and 7. False color is added to aid interpretation of image. Blue areas are clean and red areas have contaminant.

Results and Accomplishments

Development of Test Coupons

In order to evaluate the usefulness of the FTIR and laser imaging method as a cleaning verification method for DOD applications, we prepared a number of test panels during the project with well characterized levels of contamination in order to determine detection limits as a function of: (1) contaminant; (2) level of contamination; (3) degree of surface roughness; (4) effect of spectral interference; and (5) instrumental parameters such as angle-of-incidence. On the advice of our Technical Advisory Committee (TAC), five candidate materials were chosen as contaminant species for evaluation as shown in Table 1. These materials have proven to be particularly difficult to remove during cleaning operations, and are representative of many other organic contaminants encountered in the DOD. A silicone-

base mold release agent was used in order to characterize contaminants of that chemical composition. The North Island mixture consisted of four contaminants considered by North Island personnel to be common surface contaminants difficult to remove. These included MIL-L-23699 aircraft lubricating oil, MIL-H-83282 hydraulic fluid, MIL-G-81322 aircraft grease, and MIL-G-25013 silicone bearing grease.

A number of metals were chosen as substrates for the target contaminants, based on usage information obtained from military and contractor facilities. These were: Aluminum-7075-T6, Titanium 6Al-4V, Steel Alloy 4340, Stainless Steel 304, & Magnesium AZ31B. The metals were fabricated into 1.5" x 5" flat coupons for laboratory testing and method demonstration.

Six surface roughness finishes of the Aluminum 7075-T6 test coupons were obtained, ranging from 80 to 600 grit (600 grit being the smoothest). A profilometer instrument was used to examine the surface roughness profiles and provide average R_a values in micro-inches. Due to the nature of metal-shop finishing processes, surface roughness values can vary considerably across a given surface area, especially in the longitudinal versus transverse directions. The metal surfaces of the coupons, upon finishing, acquired a directional "grain" parallel to the coupons' longitudinal direction. Two surface roughness levels, 600 and 220 grit, were obtained for the remaining metal types.

Table 1 – Test materials chosen for evaluation of technique.

<u>Material</u>	<u>Description</u>	<u>Usage</u>
Safety Draw	White soft solid – ester grease	Metal drawing, cutting, and lubricating agent
Cosmoline	Brown liquid – paraffin hydrocarbons	Rust preventative, cleaner, lubricant, protectant for metals
DC4 Silicone	Translucent paste – primarily dimethylsiloxane polymer	Electrically insulating grease for lubrication
Partall Film #10	Green liquid – ethanol homopolymer	Mold release agent
North Island Mix	Brown liquid – a mixture of four hydrocarbon-ester components.	Used at NAVDEP N.I. for aircraft lubrication and hydraulics.

Prior to contaminant application, the Al-7075 coupons were cleaned with acetone and underwent sonication with a clean-rinsing aqueous cleaner. They were thoroughly rinsed and gently dried in a 50°C oven. Once cooled, they were weighed on a semi-microbalance to the nearest 0.01 mg. Two or three weighings were averaged.

Both Safety Draw and Cosmoline contaminated Al-7075 coupons were produced by two primary deposition methods – airbrushing and manual brushing. Several other techniques

were attempted, including wire-cator drawing, coupon spinning, & manual drop and spread. They were abandoned for these particular contaminants due to the superior results obtained from airbrushing and manual brushing. Three levels of Safety Draw were applied to three Al test coupons for each of six surface finishes, creating a suite of 18 panels. Airbrushing was used for all of these coupons. Varying concentrations of Safety Draw in water were prepared for the airbrush solutions. Similarly, four levels of Cosmoline were applied to four Al test coupons for each of six surface finishes, creating a suite of 24 panels. Manual brushing was used for all but the least contaminated samples, which were airbrushed. Cosmoline solutions for both techniques were prepared using a pentane solvent matrix.

All contaminated coupons were gently heated in a 50°C oven for several days to remove semi-volatile and volatile components. This served to stabilize the contaminants, allowing for quantification by weighing. Once the weights became stable, the coupons were cooled and weighed to determine the amount of contaminant present on the surface. When not being weighed or scanned, the coupons were kept in a desiccator.

The bulk samples of Safety Draw and Cosmoline (used for theoretical film thickness predictions) were prepared by adding several millimeters of material to Teflon-lined sample boats. The samples were then heated in a 50°C oven for several days to remove semi-volatile and volatile components.

The full Safety Draw sample set was measured at NFESC and Sandia using two angles of incidence for average film thickness ranging from 0.1 to 1 μm , and aluminum substrates with surface finish ranging from 600 to 80 grit. Since the surface finishing operation produced a highly directional roughness, measurements were made both longitudinally and transversely with respect to the polishing grooves. R_a values were determined at NFESC using profilometer measurements, and resulted in surface roughness values of 0.3 to 1.5 μm for the longitudinal direction, and 0.5 to 6 μm for the transverse direction.

The FTIR reflectance data were normalized using the uncoated back of a panel as a clean reference standard, and are presented as either reflectance values (0 – 1) or reflection-absorption values ($-\log$ reflectance) in the following discussion. The C-H stretching vibrations near 2900 cm^{-1} proved to be most useful in quantifying instrument response since these frequencies are well isolated from atmospheric interference due to water and carbon dioxide. However, the baseline for these reflectance data was not necessarily flat, and was often non-linear. A simple single-point measurement of intensity was therefore not sufficient to determine the instrument response function.

Optical constants (n and k) were derived for the safety draw C-H stretching vibrations using the Sandia reflectance code and dispersion model to calculate a fit to the experimental data for one of the test coupons. Reflectance-absorption spectra for the 2800 – 3000 cm^{-1} range were calculated for 1 μm thick films of Safety Draw on an aluminum surface at either 60 or 75° angle of incidence. This function was then used as a linear variable in conjunction with a second-order polynomial to produce a least-squares fit of the experimental data for the test coupons. An example is shown in Figure 9 for the longitudinal measurements of three thicknesses at a 75° angle of incidence. This procedure produces extremely rapid, robust

analyses of the reflectance data, even for the thinnest films in the presence of noise, and accounts well for baseline shifts and curvature due to interference fringes.

Fitting coefficients for the linear spectral function (which are proportional to the integrated intensity) are then plotted against the average calculated film thickness, and these results are shown in Figures 9-12 for longitudinal and transverse reflectance measurements at 75 and 60° angle of incidence. Results for the longitudinal, 60° angle of incidence follow a very linear relationship with film thickness except for the roughest surface finish (80 grit, $R_a = 6 \mu\text{m}$). Instrument response for transverse measurements at 60° angle of incidence are also reasonably linear, with the same average slope, except for the roughest test sample. The transverse data show additional scatter, when compared to the longitudinal measurements, which is not unexpected due to the large increase in surface roughness and the attendant increase in light scattering at these wavelengths ($3.3 \mu\text{m}$).

In contrast, analysis of the FTIR reflectance-absorption data at a 75° angle of incidence for both longitudinal and transverse sample orientations shows a marked departure from linearity at the highest values of film thickness (Figure 11). Initial slopes in these figures are slightly greater than the 60° angle of incidence data (Figure 10). This is expected due to the increase in reflection-absorption sensitivity with increasing angle. The transverse measurements again exhibit a larger scatter in slope compared to the longitudinal data due to the larger surface roughness encountered in these measurements. Here, too, the average initial slope (and hence instrument sensitivity) is the same for both transverse and longitudinal orientations.

The pronounced non-linearity in slope for the thickest films at 75° was unexpected, although an additional enhancement in sensitivity does occur for the reflectance-absorption of a film with increasing angle of incidence [1]. Under appropriate conditions this may cause a non-linear response for thicker films. Such an interpretation is not substantiated by calculated spectra for the present measurement conditions, however, due to the small change from 60 to 75° in angle of incidence. Furthermore, such a non-linear effect would be most pronounced for measurements on the smoothest substrate (Figures 11, filled circles) where the effective local orientation of the surface is most constant with respect to the illumination beam. In contrast, these are by far the most linear sample series for the 75° data.

We attribute the pronounced non-linearity of the 75° data for the thickest Safety Draw films to the morphological characteristics of the material as deposited on the aluminum test panel surface. As described above, Safety Draw is a highly viscous material that forms a visibly heterogeneous white film at $1 \mu\text{m}$ thickness. Variations in the deposition process produce relatively thick local areas of Safety Draw film and result in accretion of solid residue along the polishing grooves and ridges of the aluminum substrate. Under these circumstances, illumination of the surface with the FTIR beam at an angle of 75° results in shadowing by contaminant material on ridge structures for all except the smoothest (600 grit polish) surface. The 12-mm diameter focal area of the infrared beam is elongated by a factor of four

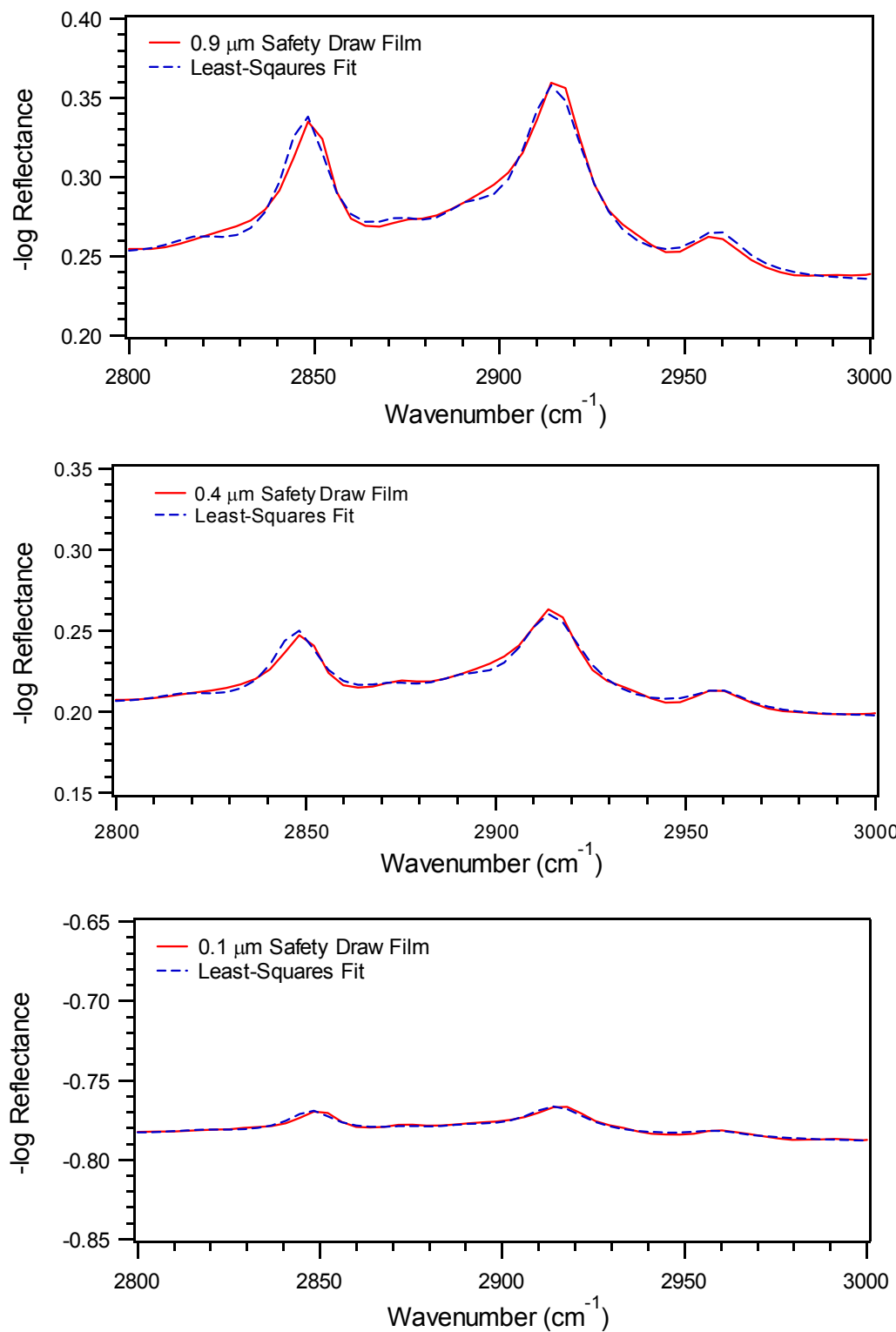


Figure 9. Linear least-squares fit of experimental reflectance-absorption data for safety draw lubricant on 600 grit polished aluminum surfaces. Average film thickness: (Top) 0.9 μm , (Middle) 0.4 μm , (Bottom) 0.1 μm .

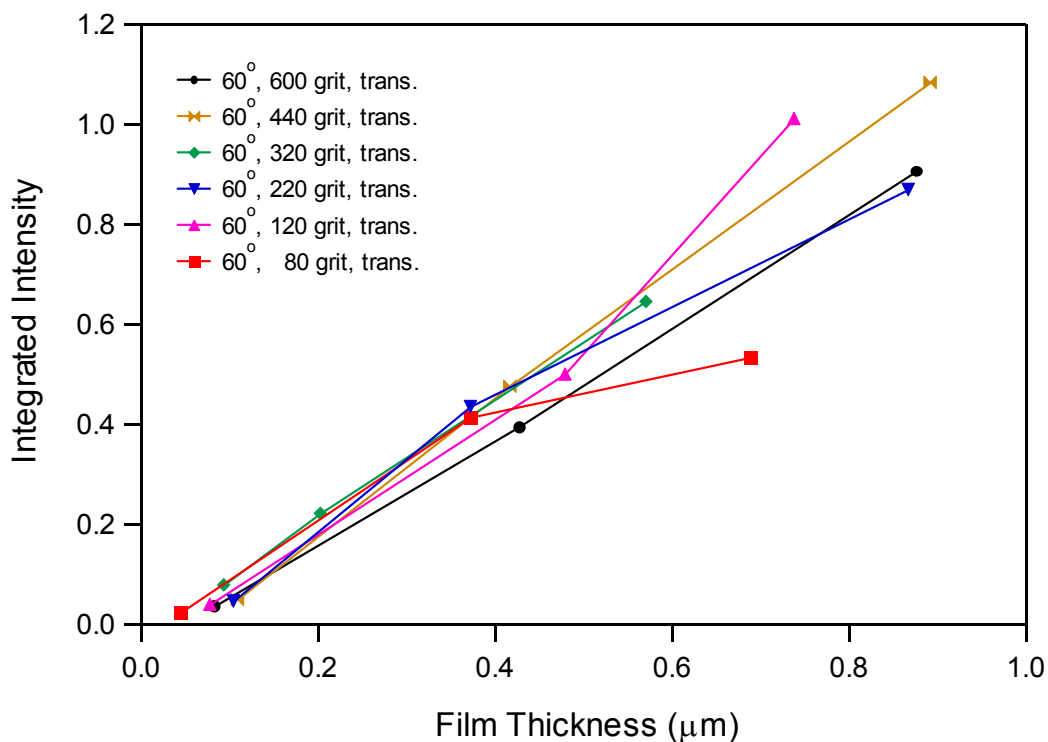
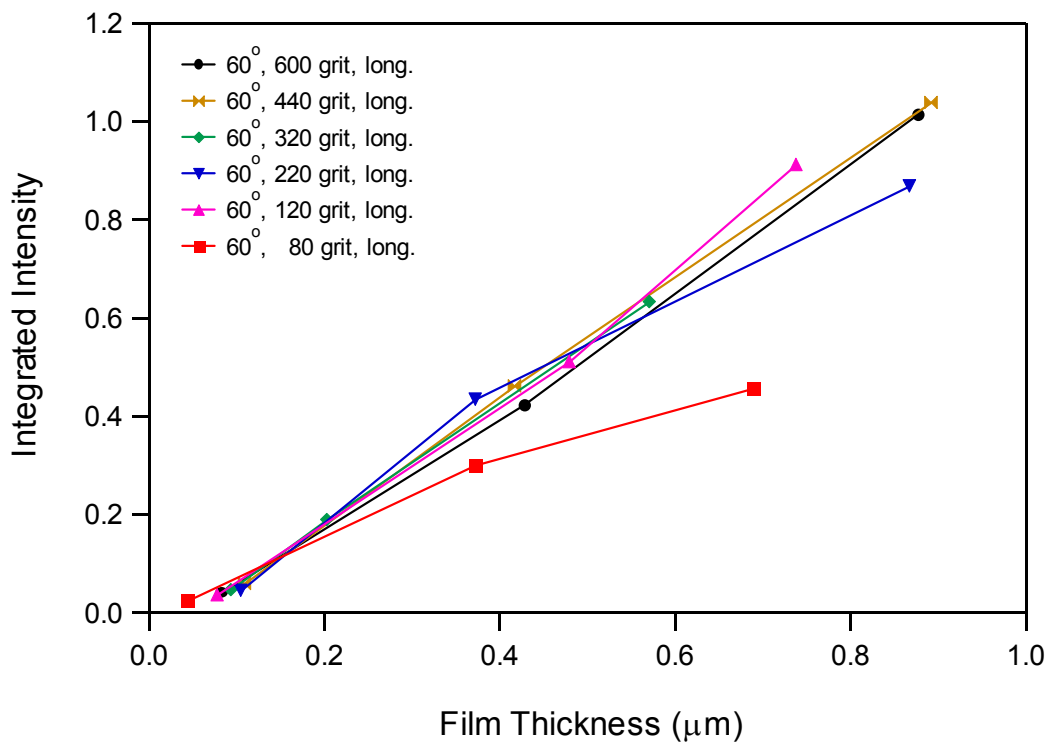


Figure 10. Integrated reflection-absorption intensity at 60° angle of incidence for C-H stretching bands of Safety Draw films deposited on aluminum test coupons with varying degrees of surface roughness (longitudinal, top; transverse, bottom).

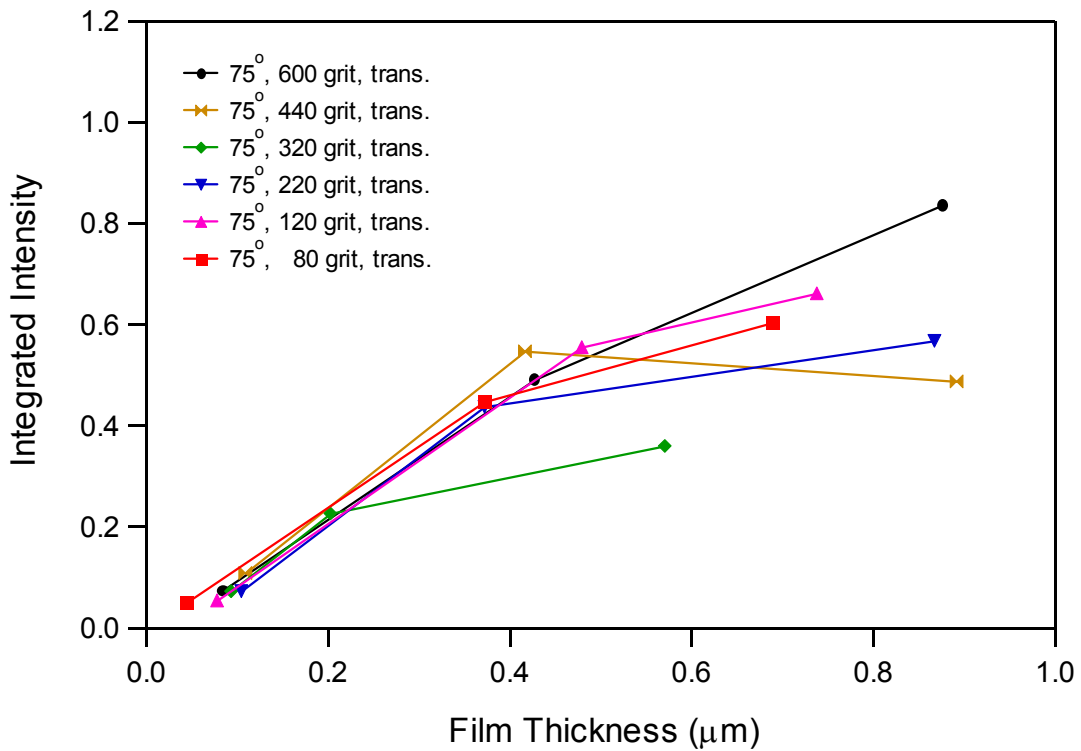
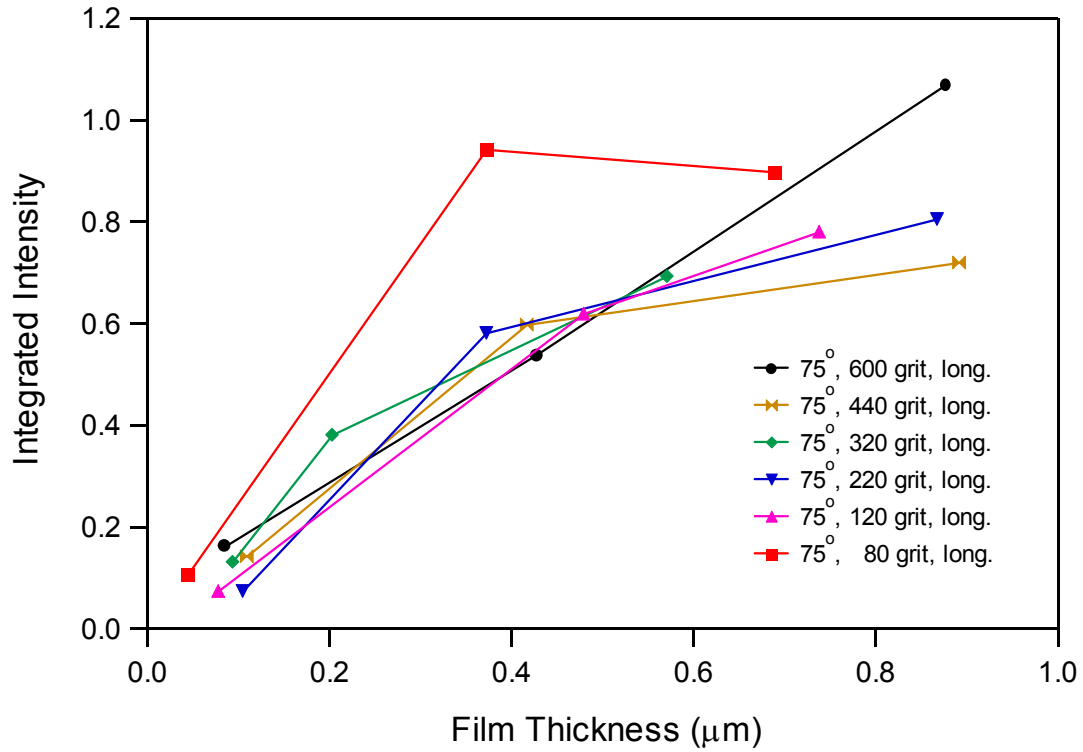


Figure 11. Integrated reflection-absorption intensity at 75° angle of incidence for C-H stretching bands of Safety Draw films deposited on aluminum test coupons with varying degrees of surface roughness (longitudinal, top; transverse, bottom).

to 48 mm for this angle of incidence. In contrast, reflectance measurements at 60° result in only a factor of 2 elongation, and minimize the shadowing effect of thick films except for ridges on the roughest (80 grit polish) surfaces.

This interpretation is substantiated by reflectance data for the second material test set (Cosmoline). FTIR reflectance measurements have been made at a 75° angle of incidence for a test series similar to that of the Safety Draw set. A preliminary analysis of the C-H stretching frequencies shows a strikingly more linear dependence of instrument response with film thickness (with the exception of a single point for one of the panels with a 220 grit surface finish). We believe that this is due to the more fluid characteristic of the Cosmoline material, which allows the deposited film to conform much more closely to the surface topography of the test coupons. These results are shown for longitudinal reflectance measurements in Figure 12.

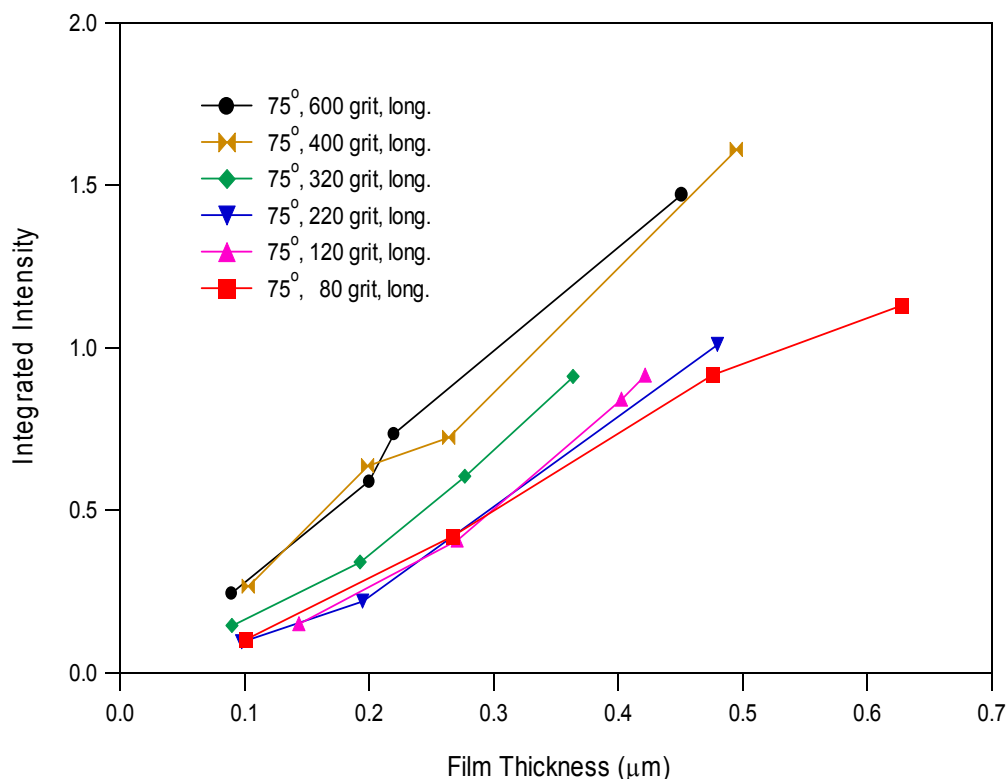


Figure 12. Initial reflection-absorption intensities of C-H stretching bands for Cosmoline films deposited on aluminum test coupons with varying degrees of surface roughness.

Throughout the project, samples were prepared at NFESC for analysis with grazing-angle reflectance by both FTIR and tunable-infrared-laser methods. The much larger bandwidth of the FTIR instrumentation provides a measure of achievable sensitivity for a variety of organic contaminants. FTIR was used to validate measurements by the laser-based instrument. In turn, the spatial resolution capabilities of the PPLN-laser imaging system can

visualize the uniformity of contaminants on prepared samples, and will aid in the quantitative understanding of spatially integrated FTIR measurements.

Based upon these FTIR studies, and experiments involving the laser-based imaging instrument, we evaluated the detection sensitivity for several classes of hydrocarbons at various laser illumination wavelengths. Based on these results, we developed a “generic” set of infrared laser wavelengths selected for maximum sensitivity in the detection of aliphatic and/or aromatic hydrocarbon species, such as oils, greases, polymers or energetic material residues.

Calibration Coupons

In September of 2001, Dr. Paul Shelley from Boeing Corp visited SOC. He brought with him two series of stainless steel calibration coupons containing ultra-low levels of polystyrene and silicone (approximately 0.8 mg/sq. ft contaminant). These coupons were prepared by NASA to be durable standards with uniform thickness levels of the applied contaminant. Dr. Martin Szczesniak of SOC analyzed the coupons on the grazing-angle FTIR prototype. Even at the lowest concentrations, which are near the detection limit of the instrument, the resulting spectra were clear enough to classify the materials. A linear progression was seen in the increasing intensity of the spectral peaks with increasing levels of contamination.

Spectral Interference

Even though excellent sensitivity was demonstrated for common hydrocarbon contaminants using infrared reflectance spectroscopy, additional concerns remained regarding the potential interference from other molecular species that may be present in the measurement environment. Chief among these was water, resulting either from the cleaning operations or the local environment. Water is a very strong infrared absorber, and its presence on the surface to be measured may cause distortion or obscuration of the characteristic contaminant reflection spectrum.

We performed an evaluation of this interference using Cosmoline test panels with an average hydrocarbon thickness of 0.7 μm on aluminum. A water film was created on the surface of the test coupon using an air brush, and reflection-absorption measurements were acquired at a 75° angle of incidence for several conditions. The thickness of the water film was difficult to determine due to constant evaporation during the reflectance measurement. We estimated the thickness by measuring coupon weight gain immediately prior to and following the infrared measurement. Film thickness was calculated based on the average weight gain.

Reflection-absorption spectra are presented for three water films on the Cosmoline test panel in Figure 13. These water films range from very thin (1 μm , not visible to the eye) to relatively thick (7 μm , clearly visible to the eye). Substantial interference is present in the 1700 cm^{-1} spectral range (not shown) due to the strong H-O-H bending mode. This obscures carbonyl absorption features that may be present in some, but not all, hydrocarbon contaminant species. The C-H stretching bands near 2900 cm^{-1} , however, are not obscured by the broad H-OH stretching bands centered near 3400 cm^{-1} . This is particularly important for the effective and accurate use of the tunable infrared-laser imaging instrument, since

images are acquired for only a small number of frequencies in contrast to the broad-band spectral data collected by the FTIR instrument.

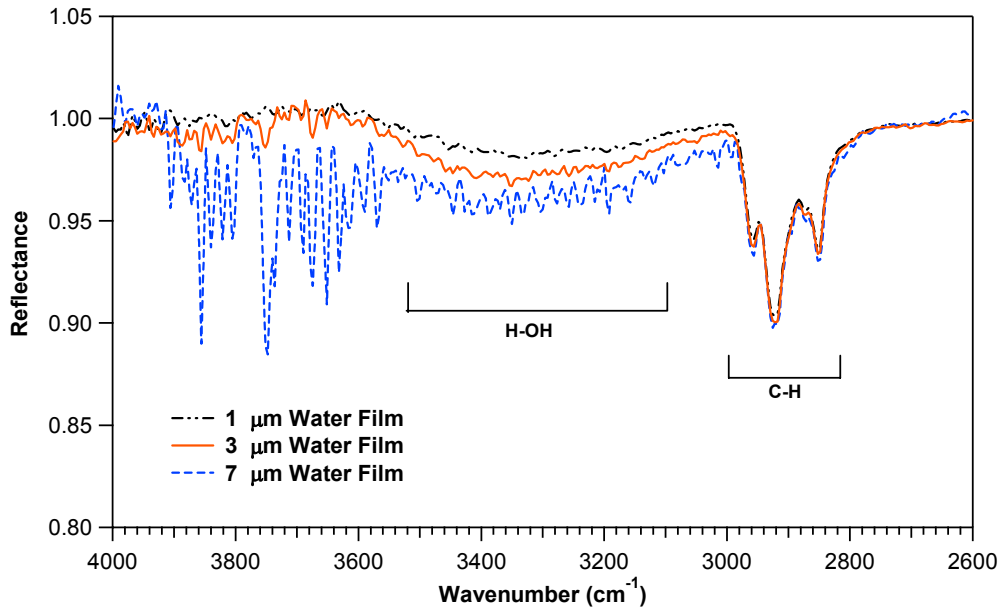


Figure 13. Potential interference effects of water on C-H stretching bands due to hydrocarbon contaminants. Three thicknesses of water film were examined (1 μm , top; 3 μm , middle; and 7 μm , bottom).

In a related problem, metallic, oxidized-metallic, and non-metallic surfaces present varying baselines. For these materials, the baseline infrared reflectance is no longer constant as a function of wavelength over the laser tuning range. This phenomenon is illustrated in Figure 14 for chromate-conversion and sulfuric anodized coatings on aluminum provided by NAVDEP North Island. The FTIR reflectance spectrum for an etched and deoxidized aluminum surface is also shown (top curve) in the figure for comparison.

Residual absorption bands near 2900 cm^{-1} due to C-H stretching modes in hydrocarbon contaminants are visible. These features are superimposed on the shoulder of a broad O-H stretching band due to hydroxyl species present in the oxide layers of the treated metal surfaces. This variation in baseline is important in the application of the laser imaging technique.

The first implementation of laser imaging used a 2-wavelength measurement technique, as described previously. One wavelength was selected to be on the C-H stretching absorption feature at $\sim 2915\text{ cm}^{-1}$, while the second laser wavelength was chosen to be one that is not absorbed by hydrocarbon residue. In this manner the second measurement could be used as a background that would account for variations in the reflectivity of the material. This technique works well for de-etched and deoxidized aluminum.

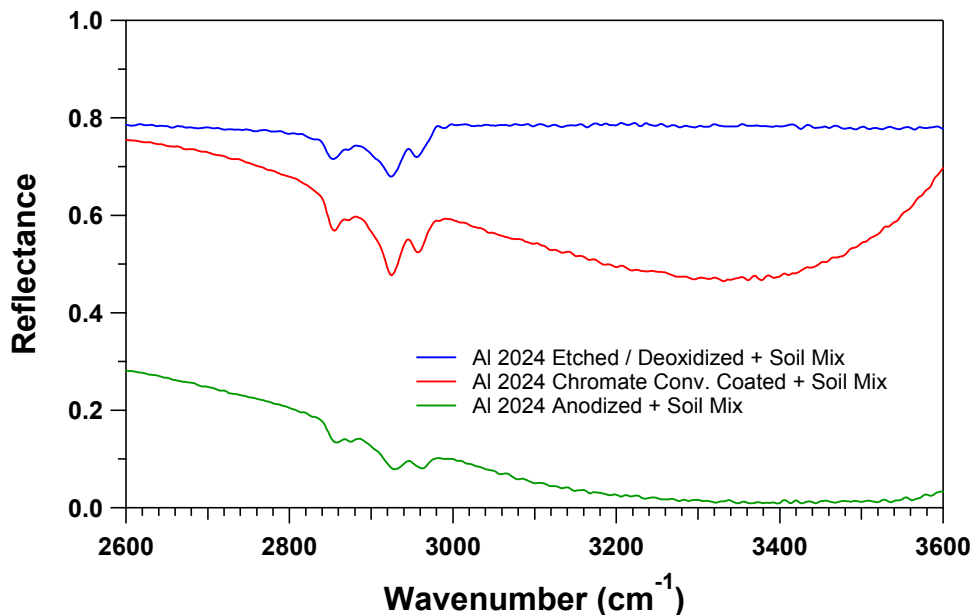


Figure 14. Comparison of infrared reflection spectra for hydrocarbon-contaminated aluminum surfaces from NAVDEP North Island (etched and deoxidized – top; chromate-conversion coated – middle; sulfuric acid anodized – bottom).

A much better approach involves a 3-wavelength measurement that establishes baseline reflectance at 2800 and 3000 cm^{-1} . In this case (and most others involving oxidized metal surfaces) a linear baseline approximation is quite accurate, and an appropriate linear combination of baseline laser images will result in an image ratio that can be accurately calibrated for residual hydrocarbon concentration. During the latter part of the project, we obtained images for hydrocarbon contamination on chromate conversion-coated surfaces in order to test this method.

NFESC prepared these variously surface-treated coupons made from Aluminum-2024 and 7075 alloy panels contaminated with the North Island soil mixture described previously and provided by NAVDEP.

Laser-image ratios for 3-wavelength measurements have been obtained for the soil mixture on chromate conversion surfaces, and are presented below in Figure 15. These false-color images represent contamination levels of 0.454, 0.315, and 0.160 μm average film thickness (or 40.5, 28.1, and 14.3 $\mu\text{g}/\text{cm}^2$ average surface deposit) for the top, middle and bottom images, respectively. The progression from heavier to lighter hydrocarbon contamination in this series of surfaces is clearly visible.

In general, the North Island soil mixture forms a very non-homogeneous layer on the metal surface. This property can be clearly seen in all three images by splotchy nature of the

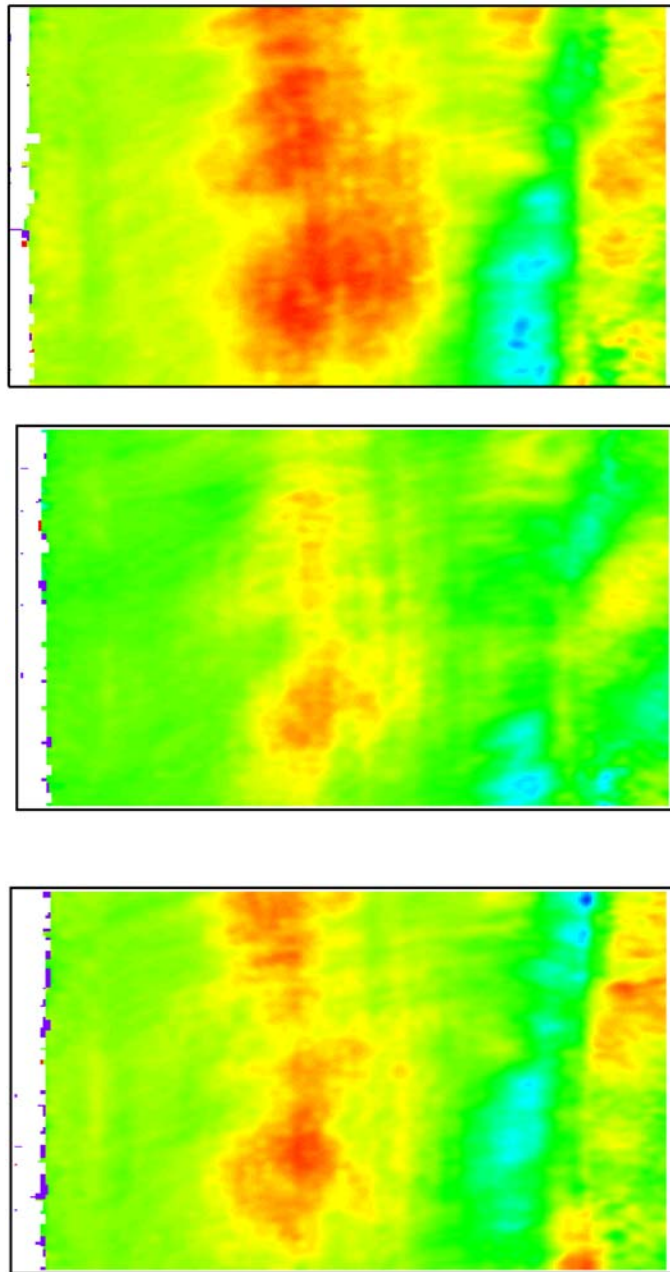


Figure 15. False-color reflectance-ratio images of NAVDEP chromate conversion aluminum surfaces contaminated with a hydrocarbon soil mixture: $40.5 \mu\text{g}/\text{cm}^2$ (top), $28.1 \mu\text{g}/\text{cm}^2$ (middle), and $14.3 \mu\text{g}/\text{cm}^2$ (bottom) average surface deposit.

images. In comparing the last two images in Figure 15 an unexpected result is seen. The bottom image represents a sample with a lower average surface deposit ($14.3 \mu\text{g}/\text{cm}^2$) than the middle image ($28.1 \mu\text{g}/\text{cm}^2$), but displays a larger contaminant spot in the image. This indicates that there is a larger deposit in the area of the bottom panel that we selected for

analysis than in the area selected for analysis of the mid-level contamination panel. The middle panel may have a higher amount of contaminant thinly spread over its surface, possibly at a level that would not hinder adhesion of a coating, while the bottom panel could have a more localized, but lower mass of contaminant that would interfere with painting the surface.

All of these hydrocarbon films are not visible to the naked eye and their spatial distribution is markedly inhomogeneous. The laser-imaging method can provide real-time assistance in evaluating the effectiveness of cleaning procedures, or the rapid localization of residual material during the examination of coating failures on DOD component surfaces.

Non-metallic or non-reflective surfaces are not well-suited to grazing-angle reflectance analysis. Non-metallic composite materials are used in a variety of DOD components. Examples include the outer skins of the E and F series of F/A-18 jets, and the F22. These aircraft contain outer skins made from graphite epoxy composites. North Island personnel described a problem experienced with these materials due to heat damage during aircraft operation. The damage is not visually detectable but a chemical change does occur which could affect the performance of the material. The current detection practice is to obtain plugs of the composite material and send them to a laboratory for TMA (thermal mechanical analysis). Successive laminated layers of the material are tested and the changes in Tg (the glass transition temperature) are tracked. This is an extremely time-consuming and costly process. The North Island personnel were seeking a better detection method, in particular a rapid on-site method.

However the reflectivity of non-metals varies widely. Non-metallic substrates that contain organic content will absorb infrared radiation and these absorptions are mixed into the resulting spectrum of the contaminant film. This reduces the overall energy that reaches the FTIR detector and complicates interpretation of the spectra. The p-component of incident radiation is not as greatly enhanced for non-metals as it is with metals. Also, the optimal angle of incidence varies with the substrate type for non-metals and may be below 60 degrees, the grazing angle threshold.

Representative non-metallic composite materials were evaluated at NFESC. The grazing-angle technique was unable to distinguish the thin film of hydrocarbon contamination applied to the composites' surfaces. Additionally, as demonstrated during the first visit to Hill AFB, a metal surface that is rendered non-reflective by a rough surface profile will be unyielding to analysis by grazing-angle reflectance. Grazing angle reflectance FTIR is unsuitable for these types of materials.

Inorganic surface contaminants, such as rust or scale, were not evaluated. The FTIR technique is capable of detecting a number of metal oxides, but analysis is complicated by the lack of available data on the optical properties of these materials. Additionally, the preparation of accurate calibration standards would be extremely difficult due to a lack of solubility for these materials.

Non-Ideal Surfaces

Many real DOD components do not have flat surfaces, but instead have complex geometries that need to be monitored. In order to determine the range of curvatures that both of the instruments could successfully monitor, a small diameter cylindrical piece of aluminum was evaluated by both methods.

A suite of six aluminum cylinders was coated with varying amounts of Cosmoline contaminant. The radius of curvature for the cylindrical samples was 1 cm. Film thickness values ranged from 0.1 to 1.5 micrometers (8 to 120 $\mu\text{g}/\text{cm}^2$). Clear, useable spectra were obtained in both longitudinal and transverse directions to the cylindrical axis using the laboratory grazing-angle FTIR optical interface.

Spectra of four of the six aluminum cylinders analyzed are presented in Figure 16. At every film thickness, the spectrum shows clearly defined C-H stretching peaks with relatively little noise in the baseline. Functional group absorbance at lower wavenumbers is well-defined for contaminant films greater than 0.2 μm in thickness (16 $\mu\text{g}/\text{cm}^2$), as compared with a sensitivity of 0.2 $\mu\text{g}/\text{cm}^2$ for flat surfaces. It is evident that the FTIR grazing angle method is capable of producing readable spectra for very thin films on curved reflective surfaces down to 1-cm radius of curvature.

The effect of orienting the samples with their cylindrical axis both longitudinally and transversely to the infrared beam is shown in Figure 17 for the 0.2- μm film sample. As expected, reflectance spectra acquired at 75° angle-of-incidence show an enhancement of absorption intensity relative to those at 60°. We observe, however, that the absorption intensities are also greater for the transverse sample orientations at both angles of incidence. This trend is the opposite behavior observed for flat test coupons above (due to the effect of increased scattering from directional polishing marks on the flat panels). Orientation effects for measurements on non-flat surfaces are due primarily to a critical dependence on sample alignment with the optical interface collection optics. The observed behavior in these measurements probably represents the relative difficulty in collecting longitudinally reflected light from the highly curved surfaces.

Peak integration yielded a reasonably linear response of the measured reflectance intensities with film thickness for these samples, as seen in Figure 18. These excellent results are due, in part, to the smoothness of the aluminum cylinder surfaces (> 600 grit). An increase in the surface roughness would be expected to result in degradation of spectral quality.

The effect of surface roughness was investigated using the Partall film #10 contaminant. Partall was applied to 1-cm radius aluminum cylinders in the same manner as the Cosmoline contaminant. Figure 19 presents integration curves for the 1735 cm^{-1} peak of the Partall spectra. The roughened cylinders (surfaces abraded with steel wool to approximately 220 grit finish) yield a slightly less intense response than the smooth cylinders.

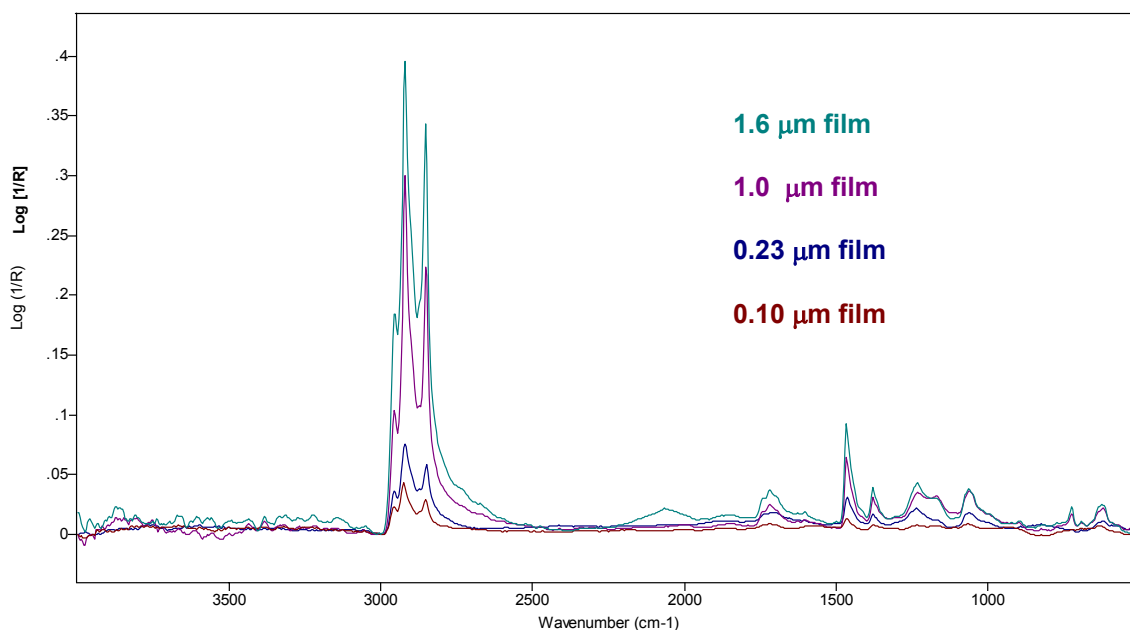


Figure 16. FTIR reflectance spectra for Cosmoline on aluminum cylinders (1-cm radius) at 75° angle of incidence and longitudinal orientation.

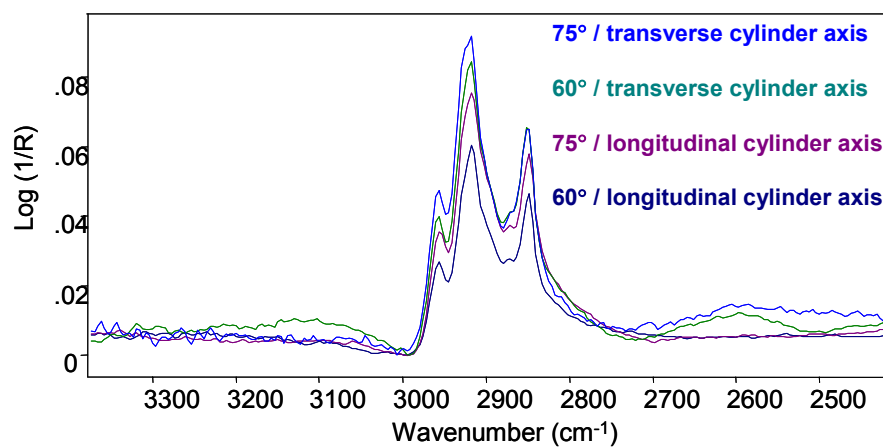


Figure 17. FTIR spectra of a 0.2 μm Cosmoline film on aluminum cylinder at 75° and 60° angle-of-incidence for transverse and longitudinal beam orientations.

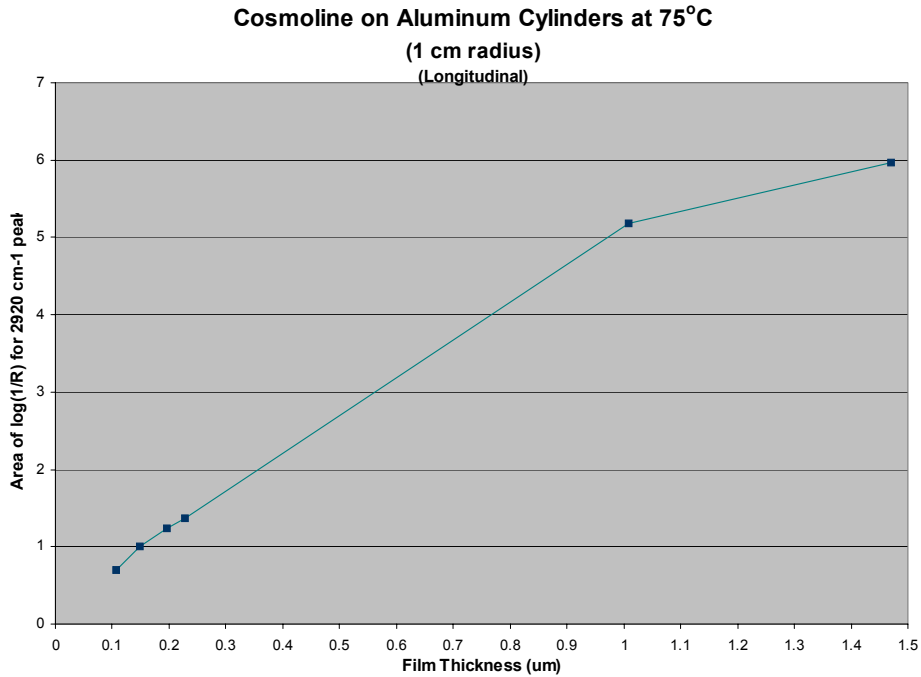


Figure 18. Integrated peak area for Cosmoline on aluminum cylinder at a 75° angle of incidence as a function of film thickness.

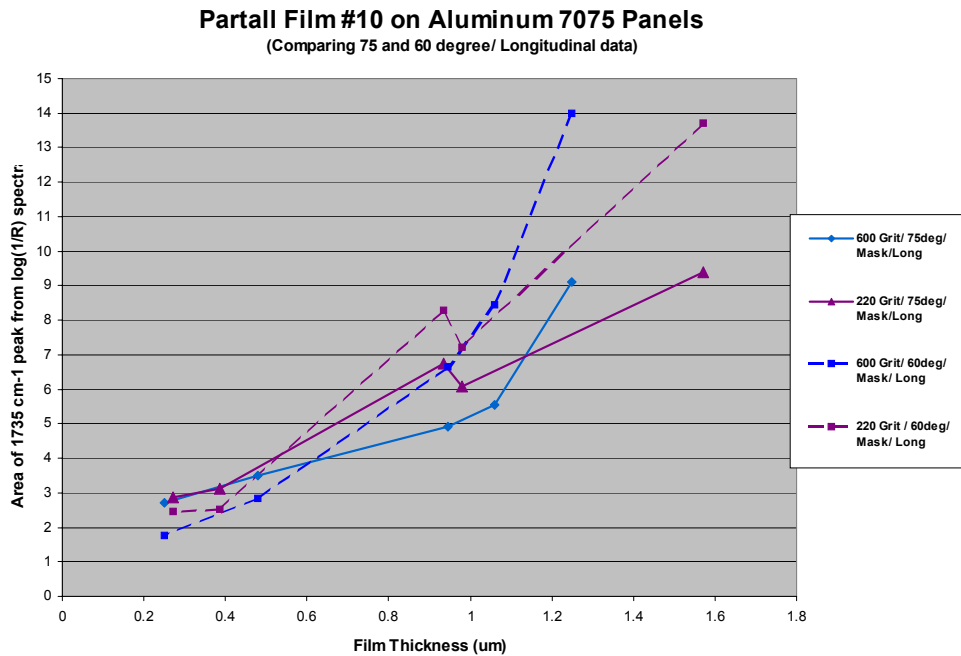


Figure 19. Integrated peak areas of the 1735 cm⁻¹ band in the FTIR reflectance spectra of aluminum panels contaminated with Partall Film #10 as a function of angle-of-incidence.

Although the instrument response function is somewhat lower than that observed for the flat panels contaminated with Partall, the analysis demonstrates that the grazing angle technique provides readable and quantifiable spectra for contaminants on curved surfaces having less than ideal surface profiles.

The same calibrated cylindrical aluminum surfaces prepared by NFESC and measured by FTIR reflectance were also examined with our tunable laser-imaging instrument at Sandia. The analogous laser-imaging measurements revealed the presence of hydrocarbons using our 2-wavelength ratio method with a reduction in the area of observation.

Since the laser light reflected from the curved surface of the cylinder diverges rapidly when the optical axis is not aligned with the cylinder axis, the most efficient measurement is obtained by aligning the incident laser illumination beam with the cylinder axis. In this case, light reflected from the curved surface is collected by the infrared camera in a band along the sample surface. Where the normal laboratory illumination area is a 21 x 35 mm rectangle, the illumination from a 1-cm radius surface results in a viewing area of 4 x 35 mm in a horizontal stripe along the center of the image. This is shown in Figure 19 for 2 cylindrical samples with average Cosmoline film thicknesses of 1.01 and 0.23 μm (or 89.3 and 20.4 $\mu\text{g} / \text{cm}^2$ average surface deposit) for the top and bottom images, respectively.

In these false-color images, heavy hydrocarbon contamination is visible along the center of the top image as orange spots, with a moderately heavy layer of contamination indicated by yellow areas. Contamination levels are a factor of 5 lower in the bottom image as revealed by a continuous green area on the left-center side of the sample surface, and several striped regions on the right-center side of the sample surface. Measurements of both FTIR and laser-imaging instruments on samples with the present radius of curvature illustrate the capability of both methods for examination of aircraft surfaces with non-flat geometry.

FTIR Spectrometer Prototype Field-test Summary

The prototype FTIR instrument exhibited excellent performance during three field trials. A few suggested improvements resulting from the first two field trials, in order to make the instrument more easily used by Air Force personnel in the field, were integrated into the design by Surface Optics Corporation. Following the completion of the modifications, an additional self-imposed field test conducted at Hill Air Force Base in Ogden, Utah, demonstrated the new ergonomic modifications. The device is now commercially available from Surface Optics Corporation (SOC) and units have been purchased by the Boeing Corporation and NASA for cleaning verification applications on aircraft and aerospace components. An additional spectrometer has been purchased by Oak Ridge National Laboratory. Based on feedback from personnel at Hill AFB and at Naval Depot North Island, SOC upgraded the prototype with more user-friendly features. SOC completed the requested upgrades in December 2001 in time for the third field test in March 2002 at Hill AFB.

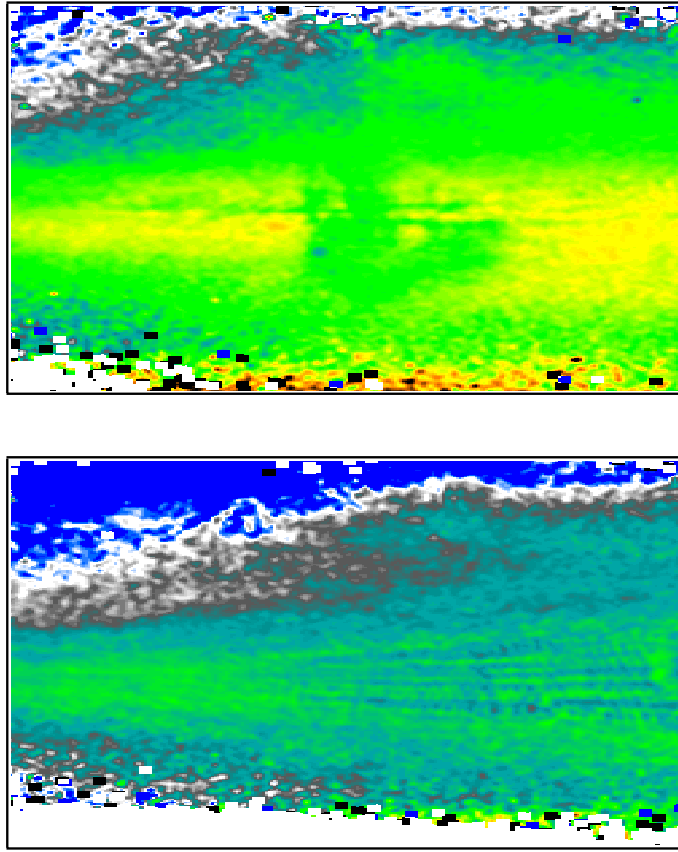


Figure 20. False-color laser-image ratios for Cosmoline contaminated cylindrical surfaces: $89.3 \mu\text{g} / \text{cm}^2$ (top) and $20.4 \mu\text{g} / \text{cm}^2$ (bottom) average surface deposit.

A number of Hill AFB maintenance personnel attended. Among those in attendance were Richard Buchi and Wayne Patterson, members of the project's Technical Advisory Committee. Figures 21 – 23 show scenes from the demonstration.

Two aircraft in the maintenance hangar were chosen for the FTIR demonstration: a C-130 and an F-16. The C-130 had been stripped to bare aluminum using plastic blast media Type V (polymethylmethacrylate). The F-16 had been stripped, also using Type V plastic blast media, to its chromic-acid anodized aluminum surface with yellow epoxy primer still present in some areas.

NFESC prepared two series of calibration coupons for the demonstration. All coupons were aluminum-7075. Three different finishes were selected. A third of the coupons were bare aluminum, another third were chromic-acid anodized aluminum, while the remaining third were dichromate-conversion coated (alodined). The coupons were further separated in two groups to receive one of two contaminants: plastic blast media Type V or the North Island hydrocarbon mixture. SOC analyzed the coupons on the portable FTIR, and created calibration curves for use during the demonstration.

The main cleanliness problem reported by Hill personnel for these aircraft was the retention of plastic blast media residue on the surfaces of the aluminum skin. This residue, if present in sufficient concentration, has been shown to be detrimental to future coating operations. The FTIR device was easily able to detect this residue on the C130, even though the calibration data suggested that its level was $< 18 \text{ ug/cm}^2$. Personnel present concurred that the upgrades to the software made the unit more user-friendly. The new software uses one-click icons and windows to direct the operator to prepare a calibration curve, analyze an area on the aircraft, and compare that contaminated area to both the calibration curve (to quantify the contaminant), as well as to a library of contaminants (to classify or identify the contaminant).

The calibration coupons prepared at NFESC contained relatively high levels of contamination, i.e. the accuracy of the calibration at the bottom of the curve ($< 10 \text{ ug/cm}^2$ contamination) was questionable. This caused a problem with one of the analyses. A negative concentration value was calculated by the computer for an unknown contaminant on the aircraft surface, based on this calibration curve. The noise in the baseline of the unknown spectrum, compounded with the problem of accuracy at the low end of the calibration curve, caused this difficulty. The solution to this problem is to obtain calibration coupons that represent a much lower range of contaminant concentration, such as those described earlier and prepared by NASA. Such coupons are more difficult to prepare and require more sophisticated techniques. NFESC coupons were prepared by a crude brush application technique. NFESC does not have the capability to produce the ultra thin uniform films. However, a number of commercial sources are available to provide this service. Once prepared, and with careful handling, calibration coupons containing the polymethylmethacrylate contaminant can be used over and over. NASA was able to prepare coupons with very low concentrations of silicone and polystyrene contaminants for Boeing Corporation. These coupons were used multiple times over the course of several months.



(A)



(B)

Figure 21. Portable FTIR analyzing (A) C130 bare aluminum belly and (B) an area containing yellow epoxy primer on an F-16.



Figure 22. FTIR operator at the C130 demonstrating handheld FTIR operation.



Figure 23. FTIR operating on a camera tripod to analyze the F-16.

Laser Imaging System Summary

The design of the imaging system included a consideration of the ultimate instrument cost and utility. The factors that influenced these design decisions were: size and weight, wavelength, commercial availability, and sensitivity.

Midway through the project it was decided that a continuous-wave system was less expensive due to the lower cost of some candidate pump lasers (such as near-IR fiber lasers) for the laser source. However, when several attempts to purchase a suitable IR fiber laser were made, the technology had not matured sufficiently to produce reliable commercial products. Since then, the commercial availability and reliability of fiber lasers has increased dramatically. Any subsequent work could easily incorporate a fiber laser as the laser pump

source. This would greatly reduce the size of the prototype cleanliness verification monitor, and ultimately the cost.

A milestone for the project was to evaluate the feasibility of incorporating a longwave IR laser that would permit spectral access to more intense features further into the IR (4-8 μm) than the current midwave-IR laser (3-5 μm). The development of the longwave laser was only begun at the start of this project and did not progress quickly enough to be incorporated into a prototype. That technology has since developed, so that it is at the point where the mid-IR lasers were when this project began. Use of a longwave IR laser would permit access to more intense features and could enhance sensitivity by as much as one order of magnitude, but would require several more years of development to produce a reliable, ruggedized version that would be suitable for field tests and/or commercialization.

Another important factor in the ease of use and cost of a laser imaging prototype is the detector type. The original laboratory system made use of an Indium-Antimonide (InSb) cryogenic focal plane array camera. The liquid nitrogen-cooled detector exhibited excellent sensitivity, but the requirement of cryogenic cooling in a field instrument was deemed prohibitive. The alternative was to incorporate a relatively inexpensive, thermoelectrically cooled silicon microbolometer array. This produced a more cost effective and portable imager component. A result of the thermoelectric cooling, however, is significantly less sensitivity than the cryogenic camera. Testing of the new detector revealed decreased sensitivity when imaging rough surfaces due to reduced light levels caused by light scattering. The improvements in camera system design should also allow observation of contaminants on rough surfaces that are commonly encountered in DOD components. The intensity of the laser source at the relevant infrared wavelengths did help to partially compensate for the loss in sensitivity of the detector.

The thermoelectrically-cooled silicon microbolometer array and software interface was constructed by Surface Optics Corporation, Inc. The integrated software permits immediate processing of the raw data images into false-color ratio images for visual analysis. The software includes the ability to use either 2 or 3 wavelength ratio images for analysis. Figure 24 depicts the silicon detector array. Figure 25 is a screen shot of the main window of the integrated laser imaging software.

Another factor in prototype design was the weight and size of the instrument. The original laboratory system made use of free space optics to guide the laser radiation to the surface and then to the detector. The inability to procure a smaller, lighter pump laser prohibited the development of a complete unit that would be compact enough and light enough for a worker to easily lift and hold in place on the surface of an airplane. In order to overcome this issue, the laser source and the detector module needed to be separated. The simplest manner in which to accomplish this was through use of a fiber optic. The fiber optic would transmit the laser radiation to a detector head assembly where it would interact with the surface under examination and then be directed to the detector array.

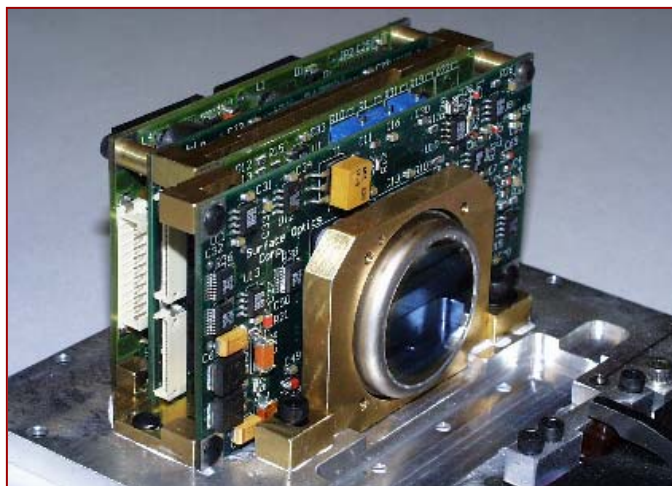


Figure 24. The new thermoelectrically-cooled silicon microbolometer array with attendant electronics.

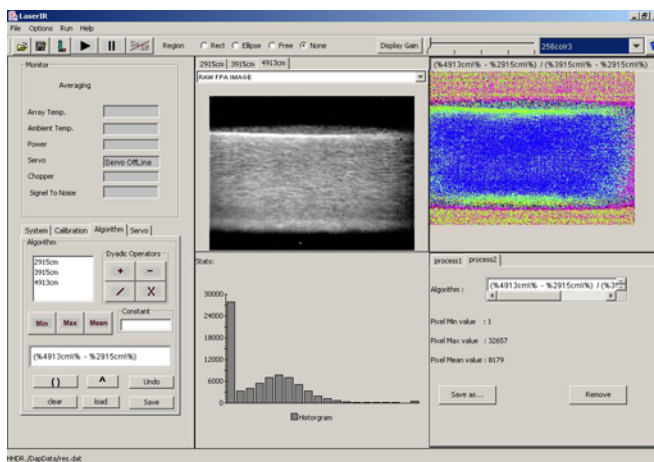


Figure 25. A screen capture of the control and data analysis software developed in conjunction with the microbolometer array.

One major issue with mid-IR fibers is brittleness and their ability to maintain their structural integrity during frequent manipulation. Since any physically weak component would render the field test instrument too delicate for its application, a number of fibers were examined prior to selection. The fiber chosen, while delicate, is not so fragile that it can not be manipulated during routine use. Further development of this instrument will require, however, that the fiber be jacketed in metal, or an even less delicate substitute identified, to increase the protection of this vital and sensitive component. The fiber port used for launching the laser into the fiber also required a custom design, although only for the lens. The standard fiber port lenses are not designed to focus laser wavelengths in the 3 – 5 μm range. While the initial fiber ports were expensive any subsequent production would drive down the cost.

The prototype constructed was laboratory tested on several calibration coupons previously mentioned as developed by NASA for Dr. Paul Shelley of Boeing Commercial Airplanes. Based upon analysis of these coupons, the laser imaging instrument was determined to have a lower detection limit of approximately 20 mg/ft².

Conclusions

The laboratory and field tests performed during this project have demonstrated that the portable grazing-angle reflectance FTIR device is a useful, valuable method for cleanliness verification of many types of contaminants on reflective surfaces. Excellent sensitivity to low levels of contaminants is observed in both laboratory and field-testing environments for a variety of contaminants on aluminum, titanium, steel alloy, and stainless steel metals used in assemblies of DOD aircraft, weapons, and other components. The instrument is capable of promoting pollution prevention by limiting the generation of waste streams through refinement and careful monitoring of the cleaning process based on feedback from the device. It also has great potential to reduce or eliminate premature failures of surface coatings caused by a lack of surface cleanliness.

Additional conclusions reached during the FTIR prototype development and field testing are given below.

A significant need exists in the military's cleaning applications for the determination of specific minimum acceptable contamination levels for each unique process. Testing of the grazing-angle device has shown that the FTIR device possesses a detection level of around 0.2 mg / ft² for many hydrocarbon contaminants. Since coating failures may occur only at higher residual contamination levels, indiscriminant use of the technique could lead to over-cleaning of component surfaces. That is, inspections with the FTIR instrument could actually lead shop personnel to over clean their parts since the device is much more sensitive to contaminants than water break testing. Therefore, a critical step in the application of the FTIR monitoring technique for each unique cleaning application is the determination of acceptable contamination levels, i.e. a pass / fail criteria to determine "how clean is clean enough" for that particular cleaning process to mitigate instrument-driven over cleaning. This might be accomplished by lap-shear tests on calibrated coupons, or by some other means. Once the threshold is established for a particular process, the FTIR software will be able to indicate whether the surface being analyzed is below or above the threshold and by how much.

In a shop environment, knowing the film thickness of the contaminant on a component's surface allows the analyst to make decisions to implement or change a cleaning process. A process that over-cleans its parts is a waste of resources, time, and money. A process that under-cleans may result in a costly and subsequent serious part or assembly failure.

Depending on the part's function, required cleanliness levels will vary. Sub-micrometer detection, for example, would be essential for determining low levels of silicone on aircraft parts. New mandatory low volatile organic content (VOC) coatings used on aircraft skins are very sensitive to silicone contaminants. These contaminants are known to leach out of door and window seals. The low levels would not be visible to the naked eye but may still require removal to prevent disbonding of the coating. Since recoating an aircraft is extremely expensive (approximately \$250K for an entire 747 aircraft), detection of the contamination beforehand is a wise approach.

Although an upgraded portable FTIR device was developed with user-friendly features, FTIR technology is still viewed as too complex by non-technical repair and maintenance personnel, preventing it from being implemented to its full potential in DOD cleanliness verification applications. The portable grazing-angle reflectance device has developed into a commercially available item and has been purchased by both commercial and government facilities. Nevertheless, DOD facilities have not, as of the time of this report, purchased and implemented the technology into their cleaning processes. During the course of the project, SERDP project members observed a reticence among shop maintenance and repair personnel to accept a tool that requires calibration, or likewise, a cursory understanding of infrared spectroscopy.

A much more common detection method used in military depots is "hexane extraction". A surface of interest is swabbed with a hexane soaked applicator, and then the dissolved surface contaminants are extracted from the solvent and analyzed. Although this detection method also involves calibration of an instrument, personnel specifically trained in spectroscopy or chromatography perform the calibration step in an off-site laboratory. At each facility visited by the project team members, however, there were always technical personnel on-site or at the activities working with the shop and depot technicians. Among technical personnel, there was a general resistance to change and a desire to continue using "tried and true" methods. Some have seen other promising prototype devices come and go and have developed a skeptical attitude towards any new device.

Additionally, having to prepare calibration coupons for a cleaning verification method may present a challenge. As indicated earlier, achieving uniform, ultrathin films requires special expertise and equipment. If the surface in question must have contamination levels $< 1 \text{ ug/cm}^2$, the coupons will likely need to be prepared by an outside organization. Depending on the contaminant though, these coupons could be stable for months if properly handled, eliminating the need for frequent purchase of preparing calibration specimens.

Finally, the problem of contaminant mixtures may lead personnel to reject the FTIR as a viable method. If the surface in question contains more than one contaminant, and no one contaminant is dominant in concentration, an accurate calibration would require the matrix to be duplicated in the reference coupons. This requires more knowledge about the contaminant matrix composition.

With time, it is anticipated that the increasing user-base for the portable grazing-angle FTIR device will lead to method developments that will make it easier for new users to utilize the

technology for their field cleaning verification needs. With continuing increase in popularity, the manufacturer will likely keep implementing improvements to the system, making it more desirable to the DOD community.

As for the laser-based system, the detector and laser system did not achieve a functional form due to time and funding limitations. The sensitivity of the detector system appears insufficient to reach the desired sensitivity in its present form. Development of the laser system was stalled for a significant period of time while construction of a smaller version was attempted from commercial parts. While that effort failed, the commercial market is now producing fiber lasers and fiber amplifiers of sufficient power in small enough packages to warrant a second look. Additionally, quantum cascade lasers (QCL) are now commercially available and might offer an alternate laser source. Also during the course of the project, IR imaging detectors have greatly expanded in availability, so alternate detector schemes are possible as well that might increase sensitivity.

Life Cycle Cost Estimate for the FTIR

A preliminary cost-benefit analysis for the FTIR prototype was discussed at the TAC meeting in October 2000 at Sandia. The initial conclusion was that the optical method could be economically feasible. A subsequent economic analysis was performed for the FTIR grazing-angle spectrometer system in response to an action item from the In-Process Review in April 2001. The analysis was performed using ECONPACK 2.0 software, a DOD economic analysis package developed by the Army Corp of Engineers. The example application considered was the refurbishment of aircraft wing panels at NAVDEP North Island, San Diego, CA. Input cost data were provided by Tim Woods (Pollution Prevention Programs at NAVDEP North Island). Additional considerations on labor rates and material costs were provided by Tom Naguy (SERDP PP/TTAWG) and the project's Technical Advisory Committee. The cost of the FTIR instrument is \$60K.

In performing the economic analysis, we calculated a Net Present Value (NPV) for both the current visual inspection method and a new inspection method using the infrared optical monitor-over the service life period of the FTIR (estimated at 8 years). A sensitivity analysis was then performed in order to determine the effect of altering various cost elements on the NPV for both alternatives. We found that labor, by far, was the most significant factor in the economic analysis. The break-even point of the analysis was achieved by reducing labor costs by **26%** using the FTIR monitor inspection method (Figure 26).

It is estimated that NAVDEP North Island processes on the order of 30 wing panels per year, of which approximately 10 are "infant mortality" coating failures due to improper surface preparation. Results of laboratory testing and preliminary field demonstrations show that the application of the FTIR could substantially reduce or eliminate these premature coating failures. We believe that a uniform application of the technique with appropriate quality control procedures should also improve the reliability of routine wing panel refurbishment, thus lengthening average lifetime and reducing associated labor costs for future maintenance. In addition to significantly reducing labor costs associated with wing panel refurbishment, application of the infrared monitoring method will also reduce a proportionate amount of

solvents and paint-contaminated wastes currently generated in unnecessary cleaning and recoating procedures.

Our work has shown that the FTIR method possesses a detection level of around 0.2 mg / ft² for many hydrocarbon contaminants. Since coating failures probably occur only for higher residual contamination levels, indiscriminant use of the technique could lead to overcleaning of component surfaces. That is, initially, inspections with the FTIR instrument could actually lead shop personnel to overclean their parts since the device is much more sensitive to contaminants than water break testing. Therefore, a critical need in the application of the FTIR monitoring technique is the development of software that allows Pass/Fail evaluation of surface cleanliness by operators who lack a detailed knowledge of spectroscopy.

However, the operator must still determine “how clean is clean enough” for a particular application. This must be done by pull tests on calibrated coupons, or by some other means. Once the threshold is established for a particular process, the FTIR software will be able to indicate whether the surface being analyzed is below or above the threshold and by how much.

We emphasize that a favorable economic analysis has been achieved for only a single application at a given depot, even with the entire burden of the instrument’s purchase price and service cost being placed on this single application. Additional savings from multiple applications of the instrument would improve the FTIR’s economic viability and substantially reduce its payback period.

Both FTIR and laser imaging techniques can be easily applied to other problem locations on aircraft surfaces. NAVDEP North Island personnel have reported that they regularly deal with problems of leaking hydraulic fluid or fuel from the seams or connectors of the fuselage and wings. These fluids contaminate the aircraft skin, leading to subsequent coating application problems. Additionally, zero or low VOC coatings are being mandated by environmental emission regulations. The reduced amount of free solvent (used as a carrier in paint formulae) is no longer able to displace or dissolve low levels of surface contamination and may lead to adhesion problems. The benefit of the grazing-angle techniques would be to set and detect a threshold for acceptable contamination when using low VOC coatings. At Hill AFB, personnel have reported that they regularly deal with contamination from plastic blast media used to strip aircraft coatings. Residue from the beads remains on the skin surfaces even after cleaning and interferes with coating bonds. Infrared monitoring methods can easily detect these plastic residues.

Feedback from analytical staff at both NAVDEP North Island and Hill AFB has been positive about the instrumental capabilities, particularly with reference to their portability and usefulness for field evaluation. The use of this technology in an earlier non-optimized version by Boeing Aircraft was able to diagnose a cleaning process problem that ultimately prevented coating failures on Boeing 747 aircraft and the attendant savings in money and additional waste generation. These examples demonstrate the additional wide range of economic impact that infrared surface monitoring methods will have for on-line cleaning inspection.

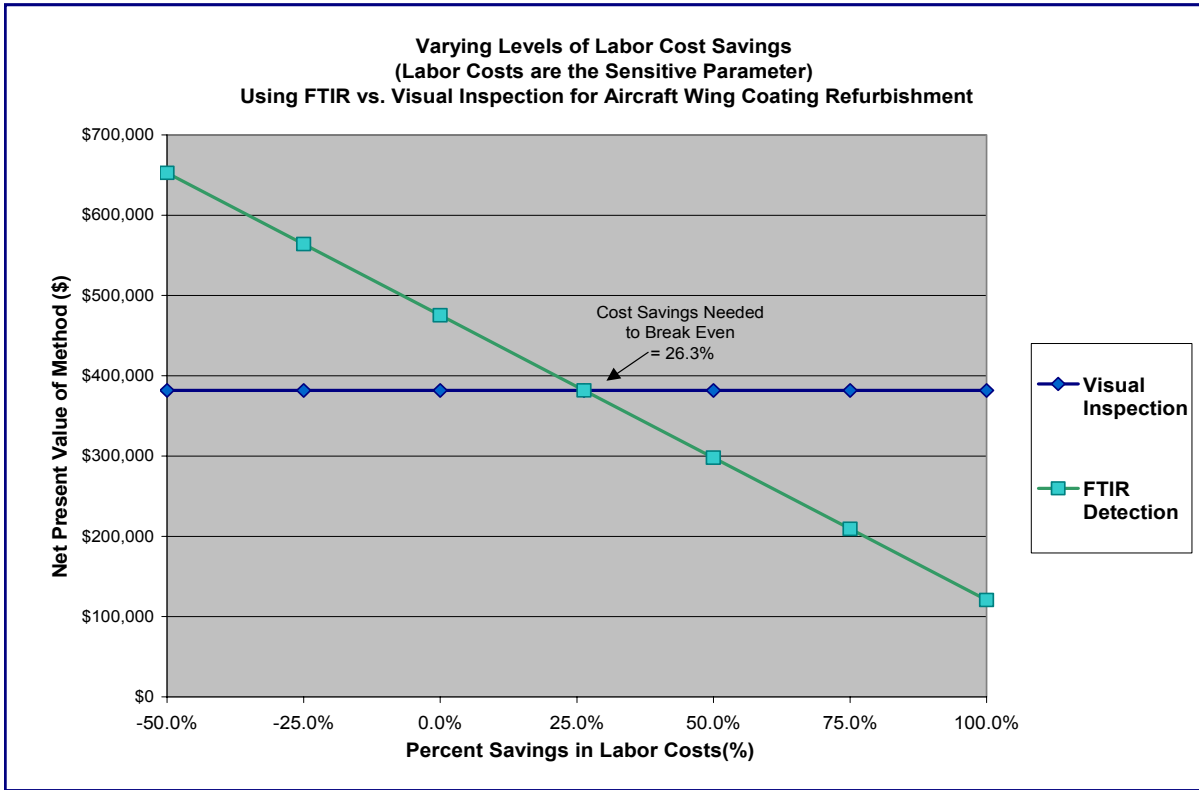


Figure 26. Economic Analysis of the FTIR spectrometer for a specific DOD cleaning application.

Transfer of Technology

As was mentioned previously, the FTIR instrument developed under this project has been successfully transferred to the commercial sector and is now available for purchase from Surface Optics Corporation as the SOC 400 Portable FTIR. The laser based system is less developed, but the development of it has continued through additional funding. Partway through this project, a second project began leveraging this work to apply the laser imaging technique to the demilitarization process of conventional munitions. The work is funded through a Memorandum of Understanding (MOU) between the DOD and the DOE and through the Defense Ammunition Center (DAC), McAlester, OK. Since many explosives are organic compounds, the CH stretch that is used for monitoring grease and oil contaminants can also be used to check for energetic materials (EM).

The energetic materials chosen as test cases were 2,4,6-trinitrotoluene (TNT), hexahydro-1,3,5 trinitro-s-triazine (RDX), and 1,3,5,7-tetranitro-1,3,5,7-tetrazacyclooctane (HMX). The energetic materials, as expected, are amenable to this detection scheme and development of the probe for this application has progressed. The program has included a test using an automated motion control system (robotic arm) to map a small area of a simulated munition interior. A field test of a manually driven control system is anticipated to occur in June or July 2004.

References

1. R.G. Greenler, *Infrared Study of Adsorbed Molecules on Metal Surfaces by Reflection Techniques*. J. Chem. Phys., 1966. **44**(1): p. 310-315.
2. D.L. Allara, *The study of thin polymer films on metal surfaces using reflection-absorption spectroscopy*, in *Polymer Surfaces*, L.H. Lee, Editor. 1977, Academic Press: New York. p. 193-206.
3. W.G. Golden, *Fourier transform infrared reflection-absorption spectroscopy*, in *Fourier Transform Infrared Spectroscopy-Applications to Chemical Systems*, J.R. Ferraro and L.J. Basile, Editors. 1985, Academic Press: New York. p. 315-344.
4. D.K. Ottesen, *An Experimental and Theoretical Study of the Infrared Reflectance of Thin Oxide Films on Metals*. J. Electro. Soc., 1985. **132**(9): p. 2250-7.
5. R.W. Bradshaw, D.K. Ottesen, L.R. Thorne, A.L. Newman, and L.N. Talerico, *Spectroscopic Characterization and Pinch Welding of Contaminated Tubing*, Sandia National Laboratories, SAND87-8241 (1987).
6. C.A. Kodres, D.R. Polly, and T.A. Hoffard, *Surface quality impact of replacing vapor degreasers with aqueous immersion systems*, Naval Facilities Engineering Service Center, NFESC-TR-2067-ENV (1997).
7. C.A. Kodres, D.R. Polly, and T.A. Hoffard, *Surface quality impact of cleaning systems*. Metal Finishing, 1997. **95**: p. 48-53.
8. D.K. Ottesen, L.R. Thorne, and R.W. Bradshaw, *Detection of contaminants in narrow-bore tubing by infrared reflection spectroscopy*, Sandia National Laboratories, SAND86-8789 (1986).
9. P.E. Powers, T.J. Kulp, and S.E. Bisson, *Continuous tuning of a continuous wave periodically poled lithium niobate optical parametric oscillator by use of a fan-out grating design*. Opt. Lett., 1998. **23**(3): p. 159-169.

APPENDIX

Appendix B: List of Technical Publications

Conference Proceeding Papers

Ludowise, P., Ottesen, D., Kulp, T., et al., "A PPLN laser-based system for chemical imaging," **SPIE Conf. On Imaging Spectrometry V**, Denver, CO, July 1999, pp. 51-59.

Ludowise, P., Robinson, S., Ottesen, D., et al., "A Laser-Based System for Chemical Imaging," **Laser Applications to Chemical and Environmental Analysis**, Santa Fe, NM, February 2000.

D. Ottesen, S. Sickafoose, H. Johnsen, T. Kulp, K. Armstrong and S. Allendorf, "Mapping of surface contaminants by tunable infrared-laser imaging," **Proc. Intl. Symp. on Surface Contamination and Cleaning**, Newark, NJ, May 2001.

T. Hoffard, D. Ottesen, H. Johnsen, T. Kulp. "Cleaning Verification Monitors Based on Grazing-Angle Reflectance Infrared Spectroscopy," **Proceedings from CleanTech 2001 International Cleaning Technology Exposition**, Rosemont, Illinois, May 2001, p. 481.

T. Hoffard, D. Ottesen, T. Kulp, H. Johnsen, and K. Armstrong. "Cleaning Verification by Innovative Infrared Optical Methods," **Proceedings from the 94th Air & Waste Management Association Conference**, Orlando Florida, June 2001.

Published Reports

Hoffard, T.A., Kodres, C., and Polly, D.R., "Grazing-Angle Fourier Transform Infrared Spectroscopy for Online Surface Cleanliness Verification," **NFESC TM-2335-SHR**, July 2000.

Hoffard, T.A., Grazing-Angle Reflectance FTIR In-field Verification, **CleanTech Magazine**, March 2001, pp. S-10.

D. Ottesen, T. Kulp, S. Robinson, P. Ludowise, U. Goers, K. Armstrong, H. Johnsen, and S. Allendorf, "Detection of Surface Contaminant Residue by Tunable Infrared laser Imaging," **SAND2001-8262**, Sandia National Laboratories, June 2001.

Published Technical Abstracts

Ottesen, D, "A Cleaning Verification Technique Based on Infrared Optical Methods," **Partners in Environmental Technology**, December 1999, p. 88.

S. Robinson, T. Kulp, D. Ottesen, U Goers, S. Allendorf, and K. Armstrong, "An Optical Method for Detecting Residual Energetic Material on Demilitarized Scrap," **2000 Global Demilitarization Symposium**, Coeur d'Alene, ID, May 2000.

Ottesen, D, "A Cleaning Verification Technique Based on Infrared Optical Methods," **Partners in Environmental Technology**, December 2000.

D. Ottesen, T. Kulp, H. Johnsen, K. Armstrong and S. Allendorf. "Detecting residual energetic material on demilitarized scrap using a laser-based monitor," **Proc. Global Demilitarization Symposium**, Sparks, NV, May 2001.

S. Sickafoose, T. Hoffard, D. Ottesen, T. Kulp, S. Allendorf, H. Johnsen, K. Armstrong, "A Cleaning Verification Technique Based on Infrared Optical Methods," **Partners in Environmental Technology Symposium**, November 2001.

S. M. Sickafoose, D. K. Ottesen, T. J. Kulp, K. Armstrong, and H. A. Johnsen. "Detecting residual energetic material on demilitarized scrap using a laser-based monitor," **Proc. Global Demilitarization Symposium**, Lexington, KY, May 2002.

S. Sickafoose, T. Hoffard, T. Kulp, K. Armstrong, J. Loomis, H. Johnsen, "A Cleaning Verification Technique Based on Infrared Optical Methods," **Partners in Environmental Technology Symposium**, December 2002.